A Phase Demodulator for Interferometric Measurements at the Head Disk Interface

Markus Staudenmann and David B. Bogy

Computer Mechanics Laboratory
Department of Mechanical Engineering
University of California
Berkeley, CA 94720, USA

Abstract

A new phase demodulator has been built which allows the direct measurement of the relative displacement between two targets. The two measurement spots may be either both on the slider, both on the disk, or one on the slider and one on the disk.

The optics from the existing BALI (Berkeley Axiom Laser Interferometer) system is used. The two reflective surfaces do not necessarily have to be almost parallel.

The phase demodulator measures the difference between the two displacements of the targets, as opposed to the measurement of two individual displacements. This reduces the number of operations necessary to obtain the spacing variation between slider and disk and therefore improves the accuracy of the measurement. In addition, a measurement range of some 100 nm is sufficient in this system, since the amplitude of the relative displacement (spacing variation and disk slope) is typically less than 100 nm, whereas the amplitudes of the individual signals are on the order of several μm. This limited range allows the application of a phase demodulation technique with high resolution.

The output of the demodulator is proportional to the difference in the lengths of the two optical paths. The spacing between slider and disk contributes to this difference as well as the thickness of the slider and the different paths through the optical elements.

The linear range of the demodulator is 0 … 316.4 nm. It can be shifted by 205 nm. This allows the reconstruction of larger displacement signals from two separate measurements.

The bandwidth of the system is DC to 1 MHz, compared to 90 kHz in the BALI electronics.

The noise level in the measurement of a spacing variation corresponds to a displacement of around 2 nm. In BALI, this value is about 10 nm.

Table of Contents

1. Introduction

This report describes the results of the project “A new Interferometer System for Dynamic Measurements of the Slider-Disk Spacing in Magnetic Disk Drives” which was funded by the Swiss National Science Foundation. The goal of this project was an improvement of the systems in CML for dynamic measurements at the head-disk interface.

The different measurement systems are presented and compared in section 2 of this report. The focus lies on interferometric systems.

Section 3 describes the new system built during this project.

The basic idea of the new system is to measure the difference between the displacement of the two target points directly, as opposed to two separate displacement measurements which are stored and later subtracted numerically. This allows the application of better demodulation techniques, since the amplitude of the relative displacement is very small (typically less than 100 nm), and a large measurement range is not required.

The main part is an electronic circuit which analyses the signals obtained from the optics used in the BALI system. This phase demodulator has a considerably lower noise level and a higher bandwidth than the electronics used in BALI.

Some measurements are shown in section 4.

The output of the new system is compared to signals from the BALI system. These signals are only examples to demonstrate the new system. Systematic investigations of dynamic effects at the head-disk interface are not presented in this report.

2. Dynamic Measurement Systems in CML

2.1. Phase Metrics DFHT

The Phase Metrics Dynamic Flying Height Tester (DFHT) is a commercial instrument which allows the dynamic measurement of the absolute flying height of a real slider, flying over a glass disk (ref. [12]). It utilizes three wavelengths interferometry (blue - 436 nm, green - 546 nm, yellow - 580 nm). The coherence length of the light is short in order to eliminate interference with reflections other than those from the lower surface of the glass disk and the air bearing surface of the slider. The spacing between these two surfaces is determined by comparing the measured light intensity, normalized after a calibration procedure, and a set of theoretical spacing/intensity curves for the three wavelengths, taking into account the complex coefficients of refraction (N- and K-value). This leads to one unique value for the spacing (see figures 2.1 and 2.2).

The spacing can be measured in the range from 1 μm down to near contact. The maximum sampling rate is 234.8 kHz, which limits the bandwidth of the system to frequencies lower than 117.4 kHz.

The main drawback of the system is the restriction to transparent (glass) disks. Measurements on actual disks are not possible with that system. Effects of disk properties, such as surface roughness or waviness, on the flying behavior of the slider can not be investigated in DFHT.

2.2. Polytec LDV

The Polytec LDV (Laser Doppler Vibrometer) allows the dynamic measurement of the motion of one measurement spot, or the relative motion between two targets. It is very easy to use, and the reflectivity of the target is not as critical as in the MCLI and BALI system described below.

Different demodulators are available:
Frequency demodulation is not accurate enough for dynamic measurements at the HDI since displacements with small amplitudes (typically less than 10 μm) at low frequencies (typically DC to ~ 200 kHz) are to be measured.
Fringe counting with interpolation allows the direct measurement of the displacement (as opposed to the velocity output from a frequency demodulator), for frequencies down to DC. However, the resolution of the best Polytec fringe counting module is still 8 nm (λ/80). This is too large to measure small spacing variations.

A second problem in the application of a commercial LDV is the size of the measurement spot. It is determined by the diameter of the laser beam, which is typically larger than 50 μm, unless

special focusing lenses are applied. However, such lenses have very short focal depth. The alignment of the optics to obtain two small measurement spots very close together is difficult.

The LDV is used in CML in various experiments. However, for the direct measurement of the dynamic behavior of the flying slider, the MCLI and BALI system described below are better suited due to their better resolution.

2.3. The MCLI System

In order to perform dynamic measurements on actual sliders and disks, the MCLI system (Multi Channel Laser Interferometer) was built in CML (refs. [10], [18]).

A laser beam (He-Ne, 632.8 nm) is directed towards the slider and the disk. Part of it is reflected off the back surface of the slider which has to be coated to be reflective (e.g. sputtered with Cr), part of it is reflected off the disk. The reflected beam is brought into interference with a reference beam. The frequency difference between the two beams is 1.25 MHz.

Two lenses are used to generate an expanded image of the target (i.e. the slider and the disk). The interference pattern at different locations in the image plane (up to 5 measurement spots) is captured by fibre optic probes and directed to photo-diodes (see figures 2.3 and 2.4).

The signals from the photodetectors are then analysed in a phase demodulator. The difference in the displacements at the individual locations leads to the dynamic spacing variation, pitch and roll motion of the slider over the spinning disk.

Two demodulators were built in CML.
One is an analog comparator (ref. [18]) which allows the real-time observation of the relative displacement between two measurement spots. Its bandwidth is 110 kHz only. The linear range is ± 80 nm. However, larger signals can be reconstructed by combination of two measurement signals (quadrature technique).
A digital phase demodulator was later implemented (ref. [10]) with a bandwidth of 278 kHz. The linear range of the electronic circuit is unlimited. The measurement range is limited only by the focal depths of the lenses and the storage capacity of the data acquisition board. However, the resolution of the digital phase demodulator is only 2.5 nm.

Since only a single measurement beam is used, the back surface of the slider has to be parallel to the surface of the disk within less than 0.1˚ in order to avoid two divergent reflections (see figure 2.5). Standard sliders do not always meet this stringent requirement.

2.4. The BALI System

The BALI system (Berkeley Axiom Laser Interferometer; refs. [6], [9]) utilizes two independent measurement beams. This eliminates the restriction to almost parallel surfaces which applies in the MCLI system. In order to keep the two measurement beams separated and brought into interference with one reference beam, a three-dimensional optical scheme was set up (see figure 2.6).

The interference pattern is coupled in two fibre optic probes which are placed either in the same image plane (if the slider is parallel to the disk) or in two image planes (if the surfaces are not parallel or if the position of the two measurement spots on the target has to be varied independently). The image plane is shown in figure 2.8. Due to the expansion of the laser beam, the diameter of the measurement spot on the target can be smaller than 5 μm (diameter of the fibres: 50 μm).

Two avalanche photo diodes detect the intensity of the light which is modulated by a carrier frequency of 20 MHz and the motion of the target.

The demodulation takes place in the phase demodulator which belongs to the ZYGO Axiom 2/20 interferometer system (ref. [20]). Either channel is demodulated independently. The phase difference between the measured intensity and a fixed reference signal is observed (see figure 2.9). In a separate circuit, the number of fringes traversing the photodetector during one experiment is counted so that no restriction to phase values smaller than 360˚ applies here. Displacements with amplitude up to 162 μm (± 81 μm) can be observed. The resolution of the phase demodulator is 2.5 nm (=λ/256).

The maximum sampling rate of the phase detector is 180 kHz, so that the highest frequency in the measurement signal is 90 kHz.

Since the measurement beam is reflected off the back surface of the slider, an absolute measurement of the flying height, as it is obtained in the DFHT, is not possible. Only the variation of the spacing during an experiment can be observed (“relative” measurement).

If the signal is disturbed due to low intensity of interference or mechanical or electrical noise in the system, “jumps” in the demodulated displacement signals occur (see figure 2.10). These discontinuities have magnitude ± 316.4 nm (=λ/2) and can be eliminated manually.

A BALI measurement is performed in the following steps (on the example of spacing variation; see also figure 2.11):

- The two fibres in the image plane(s) are positioned such that one measurement spot is on the slider, the other one is on the disk (close to the first one).
- The two displacements are measured simultaneously.
- The difference between the two displacements is calculated and stored: spacing variation plus disk runout
- The slider is moved (still loaded) so that both measurement spots are on the disk.
- The displacements at the two spots is measured
- The difference between these measurement is calculated and stored: disk runout
- The difference between the two stored signals is calculated: spacing variation

Due to the resolution of 2.5 nm, the procedure described above with 4 independent measurements and external error sources (runout not identical in the two experiments, noise in the building, etc.), the resulting noise level in a measurement is about 10 nm. It can be improved by filtering (which reduces the bandwidth) or averaging over a number of repetitive experiments.

2.5. AE sensors

An AE (acoustic emission) sensor is mounted to the arm on which the suspension and slider to be tested is mounted. The signal from the AE transducer can either be stored as raw data in the time domain, which is usually done to observe high frequencies (sampling rate 2 MHz) or as a rms-value (time constant 0.1 … 0.25 s), which is useful to determine the touch-down velocity of a certain slider-disk combination.

3. A New System

3.1. Motivation

The dynamic measurement systems in CML are described in section 2.
The two systems used most, the Phase Metrics DFHT and the BALI system, show some very nice features, but also some drawbacks.
The following table compares some of the specifications of the two systems:

System:	**DFHT**	**BALI**
Measurement	absolute	**relative**
Number of measurements	1	**4** (2 measurements at 2 spots)
Disk	**glass disk**	real disk
Slider	real slider	real slider back surface: **Cr sputtered**
Slider Motion: Vertical motion Pitch Roll	 Yes Yes (2 measurements) Yes (2 measurements)	 Yes Yes Yes
Disk Runout	no problem	to be eliminated (separate measurement)
Displacement	< 1 µm (max. spacing)	< 162 µm (max. disk runout between two fibres)
Frequency	**< 117 kHz**	**< 90 kHz**
Resolution	1 nm	**2.5 nm**
Accuracy	1 nm	**10 nm**

Table 3.1: Specifications of DFHT and BALI

Dynamic measurements on actual sliders and disks can only be performed in CML utilizing the BALI system.

However, the noise level in that system is around 10 nm in the resulting signal (e.g. the spacing variation; after the analysis of 4 measurements), which is comparable to the value of the signal itself. To obtain better measurements, the average over a number of repetitive experiments is calculated.

In addition, the sampling rate of the system allows the measurement of frequencies lower than 90 kHz only. Higher frequency components in the displacement (such as air bearing resonant frequencies, slider body resonances, disk surface effects, etc.) can not be measured.

The goal of a new system is therefore

- a smaller noise level
- a higher bandwidth

3.2. Concept

The measurement procedure applied in the BALI system (see section 2.4. and figure 2.11), where 4 signals at large amplitude are analysed independently, leads to the following:

- The measurement range has to be large (capable of measuring signals of about 10 μm), since the disk runout has to be measured together with the spacing variation
  A large range leads in general to a smaller resolution (in BALI: 2.5 nm)
- The measurement errors (electric noise, mechanical disturbances, numerical errors, non-repetitive behaviour of slider and disk) may accumulate during the process (in BALI: 10 nm resulting error).

In the measurement of the spacing variation between slider and disk, one is not primarily interested in the individual displacement of the measurement spots on the slider and on the disk, but in the difference between the two motions (relative displacement). The same is true for measurements of the pitch or the roll motion of a slider.

A new setup capable of measuring this difference directly, i.e. without measuring the two large displacements, is not required to have a large measurement range. A range of about 200 nm displacement amplitude is sufficient for most applications. This limited range allows the use of a phase demodulator with better resolution. In addition, only one difference between two signals has to be calculated so that errors in a measurement accumulate less.

In order to measure the relative displacement between two measurement spots directly, the two signals have to be combined before demodulation.

Two ways of combining the two signals are possible:

- Combination in the optical path:
  The two beams reflected off the slider and off the disk are brought into interference with each other. No fixed reference beam is utilized.
  This is realized in some of the commercial two-point interferometers such as the Polytec LDV.

Since the two measurement beams overlap on the target, a direct combination of the two beams using a half-wave plate and a polarization sensitive beam-splitter (PSBS) is not possible.

In the BALI system, small portions of the light are collected using fibre optic probes. To get interference between the two signals, the two fibres have to be brought together into one (e.g. by a fibre-optic coupler) and then led to the photodetector.

Since the intensity of the reflected light is already critical in the BALI system, the insertion of new elements into the optical path is not desirable.

In addition, the BALI system with its large measurement range and small measurement spot size should remain operational.

- Combination in the electronics:

  The two electric signals from the photodetector are combined in the electronic circuit. The optical paths of the BALI system (fig. 2.6) remain unchanged. A fixed reference beam interferes with the two measurement beams. Although only the difference between the two signals is to be analysed, this reference beam is still necessary, since the photodetectors eliminate the frequency of the laser light ($4.7 \cdot 10^{14}$Hz). Only the carrier frequency from the AOM (20 MHz) and the modulation due to the motion of the target remain in the signal.

The following table compares these two possibilities:

Combination in:	**Optics**	**Electronics**
Photo-detectors	1	2
Fixed Reference Beam	No	Yes
Light intensity	**critical**	same as in BALI
to perform BALI measurements	Change optics, realign	Change electronics (**easy**)
New elements	fibre-optic coupler	electronic gates
Resolution	same as in BALI	**?** (new electronics)
Bandwidth	same as in BALI	**?** (new electronics)
Error	70 % of BALI	**?** (new electronics)
Output at velocity = 0	0	**DC value**

Table 3.2: Combination of the two signals

Combining the signals in the optical path, the intensity of the interfering light from the two measurements spots is very weak, so that the signal to noise ratio is poor. The bandwidth of the new system remains the same as in BALI as long as the same demodulator is used. On the good side is the reduction of the number of measurements required to perform an experiment.

A considerable improvement of the BALI system can be achieved if the signals from two photodetectors are combined in the electronics.
A new phase demodulator was therefore built.

The concept of the new system is also illustrated in figure 3.1

3.3. Realization

The photodetectors each produce a phase-modulated signal with a carrier frequency of 20 MHz. The two signals are converted to square signals at TTL level. This operation is also necessary for the Axiom demodulation electronics, so that the existing comparator (AM 686) on the Axiom board can be used.

The frequency is divided down to 10 MHz, using a JK-Flip-Flop (74S112). The purpose of this division is an increased measurement range. The Axiom electronics also divides the frequency. However, the motivation there is not the measurement range, but the lower slew rates (20 MHz is high for standard TTL elements).

The frequency division for one of the signals is performed using the existing Axiom photodetector box. The other signal is divided in an identical circuit in the new electronics because a switch is to be inserted between the comparator and the Flip-Flop (see section 3.4. below).

The two TTL signals (20 MHz from Photodetector Box 1, 10 MHz from Photodetector Box 2) are transported to the new box through a pair of differential line drivers / line receivers (DS9638 / DS9639).

The generation of the input signals for the new phase demodulation circuit is schematically represented in figure 3.2.

After the second 20 MHz signal is also divided to 10 MHz, the two TTL signals are compared. A fast XOR-gate (74F86) is used as a phase detector. A logic output is generated which consists of pulses of different width, depending on the phase difference, at a rate of 20 MHz.

Note that different types of phase detectors are also possible. A digital phase detector is preferred since the output level is not affected by fluctuations in the reflected light intensity. Other than the XOR-type, also Flip-Flop, multiply-and-count, or timing-of-leading-edge types are possible to realize a digital phase detectors (see ref. [4] for details).

The carrier frequency is eliminated by means of a low-pass filter which consists of 2 RC-elements. The cutoff frequency of the filter is set to 1 MHz. This filter acts as an D/A converter, so that an analog output is available on a BNC connector at the box. This analog output is proportional to the phase difference between the two signals.

Note that the phase difference is a measure of the relative displacement between the two measurement spots, and not of their velocity. Even if the targets stand still, a DC output is generated. This is in contrast to most high-precision interferometers, where the Doppler shift f_D ($f_D = 2v/\lambda$; v = velocity v of the target) is used for demodulation.

The system is also different from other phase-demodulated systems, where the phase shift between the interfered light beams and a fixed reference signal is utilized (e.g. ref. [6], [10], [11]). In this new system, the phase difference between two interference patterns is analyzed.

The scheme of the phase detector is illustrated in figure 3.3. The main parts of the electronic circuit are shown in figure 3.4, the full circuit in figure 3.11.

3.4. Input - Output Characteristics

The transfer function of a phase detector which operates on a XOR-gate is shown in figure 3.5 a). The "output" axis is the averaged value, after the elimination of the 20 MHz carrier. The phase difference $\Delta\varphi$ corresponds to a difference Δs in the lengths of the two optical paths according to

$$\Delta\varphi = \frac{2 \cdot \Delta s}{\lambda}$$

where λ is the wavelength of the laser light (λ = 632.8 nm). A phase difference of 180° corresponds to a value of Δs = 316.4 nm. The factor 2 is due to the frequency division from 20 to 10 MHz.

Δs is caused not only by the spacing between slider and disk. It is composed of different path lengths through the optical setup (mirrors, beam-splitters, lenses, fibres, etc.), the thickness of the slider body (2x), by the slope of the disk (runout; 2x)) and by the spacing between slider and disk (2x). Zero output therefore does not correspond to a slider in contact. The DC value in a measurement provides no information on the absolute spacing.

The transfer function is linear in the range 0 … 180° or 0 … 316.4 nm. In the range 180° … 360°, the slope of the function changes sign as shown in figure 3.5 a). The whole pattern is repeated for larger differences.

If the relative displacement of the two targets is such that the signal exceeds the linear range in an experiment, the shape of the output signal depends on the DC value of Δs. This is illustrated in figure 3.5 b) for 3 different signals. Signal 3 is inverted, signal 2 is "folded" at the limit of the measurement range.

This distortion of the signal causes difficulties if the true values are to be evaluated. The input-output characteristics is therefore modified as illustrated in figure 3.6 a).

The transfer function remains linear in the range 0 … 180˚ or 0 … 316.4 nm. For higher values of Δs, this linear function is repeated, causing a discontinuity at $\Delta\varphi = n \cdot 180^\circ$. The shape of signal 3 in figure 3.6 b) remains unchanged, signal 2 shows a discontinuity as the linear range is exceeded.

This transfer function is realized by a buffer / inverter combination at the output of the XOR-gate (see figure 3.8). If the phase difference is in the range 180 … 360˚ (+ n·360˚), the logic output is inverted.

The range of the phase values is detected in a second JK-Flip-Flop (74S112; see function table in figure 3.10). One 10 MHz signal is used as the J-input, its inversion as the K-input. The other 10 MHz signal is used as the clock signal. The Q-output of the Flip-Flop remains stable at H (high) as long as the phase difference is in the range 0 … 180˚, and at L (low) for 180 … 360˚ (+ n·360˚). This signal is used to select either the buffer (74F125) or the inverter (74F366) at the output through their Tri-state input.

If the phase difference Δφ in an experiment changes from values lower than $\Delta\varphi = n \cdot 180^\circ$ to higher values, or vice versa, the output signal is distorted as can be seen on signal 2 in figure 3.6 b). This is also the case with signal 2 in figure 3.5 b) where the transfer function is not modified.

To allow the direct measurement of signals such as signal 2, the measurement range can be shifted by 205 nm. The linear range is then 205 … 521.4 nm rather than 0 … 316.4 nm, as illustrated in figure 3.7. Signal 2 is now measured without distortion, signals 1 and 3 exceed the linear range and show high-low jumps in the output (see also section 4.4. “Measurement of Large Signals”).

This shift of the measurement range is realized in a double-pole / double-throw switch, which is inserted between the line driver (DS9638) in the photodetector box 2 and the line receiver (DS9639) in the new circuit (see figure 3.2). This switch interchanges the two wires. This inverts the 20 MHz TTL signal. The output of the JK-Flip-Flop is then a 10 MHz signal which is shifted by (ideally) 90˚. Due to the time delay in the switch, the resulting phase shift is 116.6˚ rather than 90˚, which corresponds to a 205 nm shift of the measurement range.

Note that the output is, at first, always interpreted as values between 0 and 316.4 nm. To obtain the actual values, the shifts of 205 nm or 316.4 nm have to be considered.

3.5. Signal Stabilization

The output of the second JK-Flip-Flop used for the buffer/inverter selection, as described in the previous section, can also be used for a signal stabilization.

If the intensity of the interference pattern which is detected by the photo-diodes is weak, errors in the A/D-conversion in the comparator and in the subsequent frequency division occur. This is illustrated schematically in figure 3.9.
A small light intensity causes a delay in the 10 MHz output (figure 3.9 b).

If the signal from the photodetector is too small to reach the switching level of the comparator, a pulse in the 20 MHz signal is omitted. The 10 MHz signal is then shifted by 180 ˚ (figure 3.9 c). This inverts the resulting analog output signal for the displacement.

The effects of these two error sources are minimized by setting the switching level to the center value of the interference signal.

An inverted output signal is also obtained if the 20 MHz signal from the photodetector is disturbed by high frequency noise (figure 3.9 d).

These errors generate “jumps” in the displacement signal from BALI (see figure 2.10). Since their magnitude is always ± 316.4 nm, they can be eliminated from the signal after the experiment.

In the new demodulator, the last two errors c and d (with the latter being the most common in actual measurements), generate a change from H to L at the Q-output of the second JK-Flip-Flop. This output can be fed back to the preset (PR) input of the first Flip-Flop, which is used as the frequency divider. A logic value L immediately resets the output to H, independent of the CLK input, and suppresses the toggling until the error is corrected.

A switch (“Switch 1” in figure 3.10) allows this automatic signal stabilization to be turned off. The PR-input of the Flip-Flop is then tied to H. This is desirable if the signal is large so that it exceeds the linear measurement range.

A second switch (“Switch 2: Channel Selector” in figure 3.10) determines if the signal is to be stabilized in the range 0 … 180˚ or in the range 180 … 360˚ (+ n·360˚).

3.6. Calibration

The calibration of the phase demodulator is performed by comparing measurements from the BALI system to the corresponding signals from the new circuit. Since the optics remains unchanged, the very same relative displacement is measured using the two systems. The same pulse from the spindle controller is used as a trigger signal to start the two measurements.

The calibration factor is determined to be **111 nm/V**.

The output voltage (in [V]) has to be multiplied by a factor of 111 in order to obtain the relative motion between the two targets (in [nm]). The fact that the change in the length of the optical path is twice the relative motion, is already taken into account.

Some remarks:

- The signal obtained from the BALI system has always zero average, whereas the signal from the new demodulator can show a DC offset. This is due to the different demodulation schemes: BALI measures the variation of the target position, the new system measures the path difference as an absolute value.
- Using the BALI system, one can “reshuffle” the relative displacement. This is necessary because the multiplexer in the electronics sometimes misinterprets the two channels (“Fibre 3” and “Fibre 4”).
  The reshuffling not only inverts the relative measurement, but also shifts one of the two signals by one data point before the difference is taken ($x_{n+1} - y_n$ instead of $y_n - x_n$, where x_n and y_n are the n-th element of the digitized displacement signals from the 2 fibres).
  This results in a signal which shows a similar shape, but different amplitude.
  To decide which of the two signals is correct, the measurement can be performed at lower sampling rate. One signal (the correct one) remains unchanged in its amplitude, the other one changes significantly.
- The resulting signals from BALI and the new system may be inverted. For comparison of the two signals, this can later be corrected in the computer.
- Best results are obtained if the signal is about in the centre of the measurement range, i.e. if the DC level of the output is about 2 V.
  This can be achieved by shifting the measurement range (see section 3.4.), or by slightly tweaking the elements in the optical path.

3.7. Accuracy

In order to determine the accuracy of the new phase demodulator in comparison to the existing BALI system, the following procedure was chosen:

- A large number of identical experiments was performed.
- The output of the two systems was stored.
- The average over all experiments was calculated.
- The difference between each individual experiment and the average signal was calculated.
- The average of this resulting signal was zero (or a very small value).
- The standard deviation is a measure of the noise level in the signal.

The result of this series of experiments is:

- **BALI**: Noise level **< 10 nm**
- **New system**: Noise level **< 2 nm**

This procedure measures only the magnitude of random errors (“noise”) which can be eliminated by averaging. Systematic errors in the measurement (such as vibrations from the air spindle, etc.) remain in the signal.

The improvement of the signal quality can also be seen in the measurements in section 4.

The same value for the accuracy (noise level < 2 nm) was also obtained by measuring a resting target (disk on the spindle, but not spinning). Since this is not possible with BALI (the spindle controller trigggers the data acquisition there), the method described above was applied for a direct comparison of the two systems.

3.8. Drift

The stability of the measurement over a longer period was investigated capturing the relative spacing between two measurement spots on a disk which was not rotating, so that only a DC signal (plus noise) was measured. It was found that the DC level decreased at a rate of **about 6 nm per hour** (higher in the beginning; see figure 3.12).

This variation in the output can be caused by drift in the electric circuit, and also by actual changes in the length of the optical path (due to sagging, thermal expansion, etc.).

If DC measurements are performed over a long period of time, this drift has to be considered. For dynamic measurements, such as spacing variation over few revolutions, this DC shift is not a problem.

3.9. Specifications

The specifications of the new phase demodulator are summarized and compared to the BALI system in the following table:

	Zygo Electronics	**New Phase Demodulator**
Measurement Range	**< 162 μm (p-p)** (each measurement spot)	**0 … 316.4 nm** (or 205 … 521.4 nm) (+ n·316.4 nm: repetitive) (difference between measurement spots)
Bandwidth	**< 90 kHz**	**< 1 MHz**
Resolution	2.5 nm	?
Noise Level	**< 10 nm**	**< 2 nm**
Light intensity	critical	less critical than in BALI due to signal stabilization
Output	digital directly stored in PC	analog stored in oscilloscope transferred to PC
Output at velocity = 0	0	DC value
Additional Instruments	Signal Generator Axiom 2/20 electronics	 New electronics Storage Oscilloscope
Calibration	automatic	**111 nm/V**
Software	package to control data acquisition and processing	program for transfer between Data 6000 and PC

Table 3.3: Specifications of BALI and the new Phase Demodulator

4. Some Measurements

4.1. Disk Slope

The measurement of the “disk slope” (relative motion between two measurement spots on the disk) using the BALI system requires the measurement of two large signals and the calculation of the difference.

The new system allows the direct measurement of the disk slope. This reduces the noise level in the measurement.

The results from an experiment using the two systems are shown in figure 4.1.

4.2. Spacing Variation

To measure the spacing variation between slider and disk, 4 displacements have to be measured in the BALI system. The difference between pairs leads to two relative displacement signals. The spacing variation is obtained by calculation of another difference.

Using the new system, two relative displacements are measured. The spacing variation is the difference between the two.
Since the number of operations is reduced, measurement errors accumulate less than in the BALI process.

An example of an experiment using the two systems is shown in figure 4.2.

4.3. Landing Curve

Landing curves can be obtained in two different ways:

- The spindle slows down during the experiment. The relative displacement between the targets (slider and disk) is measured.
  The sampling rate of the digital storage oscilloscope is set to a low value in order to avoid too high a number of data points. This reduces the bandwidth of the system, so that high frequency variations of the spacing are not measured.
  The signal is then smoothed in order to eliminate the variation within the individual revolutions of the disk.
- The relative spacing is measured at a constant linear velocity. The average value (DC offset) of the signal is measured. By varying the rotational speed, the relationship between flying height and linear velocity is obtained.

An example of a direct measurement is shown in figure 4.3.
The landing curve is approximated by a polynomial function. This eliminates the large amplitudes caused by the disk runout.

The second way of obtaining a landing curve is illustrated in figure 4.4. The disk rotates at a constant rpm-value, the measurement is performed over few revolutions at a high sampling rate (>100 kHz). The DC-offset of the signal is read out and stored together with the rotational speed.
However, this method is not very accurate. This is shown in figure 4.5 where no slider was present. Even though the runout of the disk generates a relative displacement signal, the “flying height” should be constant for all rotational speeds. The scattering of the data points shows that an error of about 3 to 5 nm has to be considered in this measurement.

An example of the two landing curves, obtained by the two ways described above, is shown in figure 4.6.

In either case, the output function does not provide the absolute value of the flying height. Only the difference between data points can be used.
To obtain absolute values, the BALI signal is shifted to match the result of a DFHT measurement at high velocities where the influence of disk properties to the flying height is small.

Note that inner and outer edge of a slider are reversed between the BALI system and the DFHT, because BALI uses the upper, DFHT the lower surface of the disk, which spins counterclockwise in either case.

4.4. Measurement of Large Signals

It was shown in section 3.4. that the linear range of the phase demodulator is 0 … 316.4 nm. Although the measurement range can be shifted to accommodate signals with different DC levels, amplitudes larger than 316.4 nm can not be measured directly. However, such signals can still be captured if two measurements are performed as shown in the following.

The displacement shown in figure 4.7. exceeds the measurement range.

If such a displacement function is measured, the output of the phase demodulator is the signal referred to as “M1” in figure 4.8 a). The “jump” from the low to the high end of the measurement range, which is expected as the displacement curve crosses the value 316.4 nm, does not show as a jump, but as a rather smooth transition. This is due to the low-pass filter which prevents rapid changes in the output.

Since the input - output relationship is repetitive, the output function can be shifted by 316.4 nm, as shown in figure 4.8 b). The two displacements generate the same output signals.

The measurement is repeated with the shifted range (linear in 205 … 521.4 nm instead of 0 … 316.4 nm). The output is then shifted by 205 nm (referred to as “M2” in figure 4.8 c).

The three measurements can be combined manually (see figure 4.8 d). The result is the complete displacement signal shown in figure 4.7.

The signal shows a decrease in the relative spacing as the disk slows down. After about 4 seconds (corresponds to 6000 rpm), the signal starts to “oscillate”. This is due to the variation in the relative spacing in every revolution of the disk, which was eliminated at higher rpm in the low-pass filter (cutoff frequency in this experiment set to 20 Hz). To obtain a nice landing curve, the measurement data has to be post-processed, i.e. the variation in a single revolution has to be eliminated by filtering, smoothing or averaging.

Another way to measure this landing curve is again the combination of several measurements at constant rotational speeds. This result is shown in figure 4.9.
The DC levels from the individual signals have to be corrected by 205 or 316 nm.
This way is possible only if the displacement signals at each linear velocity do not exceed the measurement range for a fixed setting of the demodulator (0 … 316 nm; 205 … 521nm; 316 … 632 nm; etc).

Note that the flying heights shown in the figures 4.7 and 4.9 are larger than one would typically expect. The difference between the highest and lowest velocities is almost 300 nm.
This behaviour can partially be explained by the very high linear velocities (40 m/s).
However, it was found that the air bearing surface of the slider (50 % “nutcracker” slider) used for these experiments is damaged. In fact, the ABS is so badly scratched that a measurement using the Phase Metrics DFHT was not possible. It is obvious that such a damage highly affects the flying behaviour of the slider.

The low-to-high transition in measurement M2 looks quite different from that in M1. The signal shows a high “noise” level for time values between about 3.5 and 8 seconds.
This can again be explained by the low-pass filter: The variation in the displacement signal over one revolution, due to disk runout and spacing variation, is about 70 nm (p-p). As soon as the peaks in the signal exceed the measurement range, the output has to jump from low to high, and back to low if the displacement is back in the measurement range. This fast transitions are filtered out, so that only an “average” value remains in the signal. This value can not be analysed in this transition region. As an example, assume a signal which oscillates around the limit of the linear range (i.e. $s(t) = 205\text{nm} \pm ds(t)$, in that case). The filtered output of the demodulator then corresponds to a value of $s = 474$ nm (central value of the measurement range), rather than 205 or 521 nm!
Such transitions occur during a very long period in the measurement M2, since the displacement signal crosses the limit of the measurement range at a very small angle. This explains the duration of the low-to-high transition in M2. Only values for $t<3.5$ and $t>8$ seconds may be considered.

Measurement M1 does not show this effect so clearly because the transition occurs at higher rotational speeds, so that higher frequencies are important in that region. These high frequencies are attenuated more in the low-pass filter than those in M2 at lower rpm.
In addition, the transition in M1 occurs at a larger angle so that its duration is much smaller.

The transition if the signal exceeds the measurement range is illustrated in figure 4.10.

5. Outlook

The new system reduces the noise level in a spacing variation measurement from about 10 nm (BALI system) to 2 nm. The bandwidth is extended from 90 kHz to 1 MHz.

Further improvement of the new system could possibly be achieved as follows:

- The system could be modified such that the two measurements M1 and M2 (unshifted and shifted range; see section 4.4.) can be performed simultaneously. Part of the circuit has to be duplicated for that purpose. Two analog outputs are available then.
- The electronic circuit used for the avalanche photo diodes can be improved. A better alignment of the elements with nicer connections and soldering joints would help to reduce the noise level in the signal.
- Additional measurement channels can be implemented. The optical setup remains unchanged. Only a fibre optic probe, a photodetector and a small electronic circuit has to be added for each additional channel.

  Four measurement channels allow the simultaneous measurement of all the components of the slider body motion (spacing variation, pitch and roll motion) in a single experiment.
- The effect of the disk slope on the measurement of the spacing variation can be minimized if three measurement spots are used (one on the slider, two on the disk; equally spaced).

  The difference between the two disk measurements is due to the disk slope only. The measurement of the spacing variation between slider and disk is affected by (almost) the same disk slope, but with a small time-delay. Thus, the disk curvature can be taken into account without performing two subsequent experiments.
- The system could be modified so that “up” and “down” sliders can be investigated.
  This is achieved if the orientation of the mounting arm and the direction of disk rotation can be inverted.
- The measurement range could be adjusted automatically using an extended electronic circuit which detects the current spacing value, without considering the high-frequency variations.
- The same effect could also be obtained by means of a mechanical system. One element (e.g. a mirror) in one of the two optical paths can be moved (e.g. by a piezo-electric element) such that the relative displacement between the two targets is always within the linear range. Due to the limited bandwidth of such a mechanical system, the mirror can only follow the low-frequency components of the displacement. The high frequencies remain in the output of the phase demodulator. The measurement can then be composed of the control signal for the piezo-electric element and the demodulator output.

- By positioning several measurement spots on the slider, the elastic deformations of the slider body can possibly be observed. Due to the very small amplitudes of these motions, careful signal analysis has to be performed (modal analysis after filtering and averaging).

- Since the system allows also very accurate static measurements, it might be used for an (indirect) determination of the absolute flying height.

  The absolute flying height can be obtained if the distance between the back surface of the slider and the disk surface is known as well as the thickness of the slider body at the same position and the orientation.

  The former is determined as described in section 4.2. “Spacing Variation” of this report. The latter can be measured if one measurement spot is placed on the rear surface, one on the air-bearing surface of the slider.

  The uncertainty of n·316.4 nm (with n being an integer number), which remains in the measurement, can be eliminated since the absolute flying height is expected somewhere between 0 and 100 nm. One can subtract 316.4 nm from the measured value until a value in this range is obtained.

  Two major problems have to be solved for the measurement of the absolute flying height: The reflectivity of the air-bearing surface and the calibration.

  Since the reflected laser beam is expanded, the back surface of the slider has to be sputtered (with Cr) in order to get sufficient light intensity. A sputtering of the air-bearing surface is not desirable. However, the ABS is smoother than the back surface, so that its reflectivity is better and might provide enough reflected light intensity even if it is unsputtered.

  The system has to be calibrated to consider the different lengths of the two optical paths if absolute measurements are to be performed (if only the variation of a signal is studied, the DC level is not important). This calibration requires an element where the thickness is known with nanometer precision. Effects such as thermal expansion have to be considered. A plate of a material with very small thermal expansion (e.g. Invar) in combination with a static high-precision instrument (e.g. Zygo NewView 100) might solve this problem.

  In a measurement of the absolute flying height, the surface roughnesses of disk and slider play an important role. The influence of the surface topography on the measured spacing values depends on the size of the measurement spot and the bandwidth of the system.

  It is to be defined yet what the “absolute spacing” between the two rough surfaces is.

6. Literature

[1] C.J. Bair:
EXPERIMENTAL STUDIES OF DISK WAVINESS EFFECTS ON PROXIMITY AIR BEARING SLIDERS;
CML Gold Report 96-003, M.S. Project Report, December 1996.

[2] C. Bedoy, D.B. Bogy:
EFFECTS OF DISK SURFACE ROUGHNESS ON THE FLYING CHARACTERISTICS OF QUASI-CONTACT SLIDERS;
CML Blue Report 96-005, February 1996.

[3] C. Bedoy, D.B. Bogy, et. al.:
SURFACE ROUGHNESS EFFECTS ON FLYING CHARACTERISTICS OF PROXIMITY RECORDING HEADS;
IEEE Trans on Magnetics, Vol. 32, No. 5, pp. 3660 - 3662, September 1996.

[4] R.E. Best:
PHASE-LOCKED LOOPS: THEORY, DESIGN AND APPLICATIONS;
McGraw Hill, New York, 1984.

[5] R.J. Blanco:
HEAD-DISK INTERFACE DYNAMICS OF A PROXIMITY AIR BEARING SLIDER WITH VARIOUS DISK SUBSTRATES AND FLEXURE-GIMBAL DESIGNS;
CML Gold Report 95-007, M.S. Project Report, December 1995.

[6] M.J. Donovan, D.B. Bogy:
A NEW LASER INTERFEROMETER FOR THE SPACING MEASUREMENT OF NON-PARALLEL SLIDER AND DISK SURFACES;
CML Blue Report 94-013, July 1994.

[7] M.J. Donovan, D.B. Bogy:
EXPERIMENTALLY OBSERVED ROUGHNESS EFFECTS ON THE AIR BEARING IN THE PSEUDO-CONTACT SPACING REGIME;
IEEE Trans on Magnetics, Vol. 31, No. 6, pp. 2994 - 2996, November 1995.

[8] M.J. Donovan, D.B. Bogy:
ROUGHNESS EFFECTS ON THE AIR BEARING IN THE NEAR-CONTACT REGIME;
CML Blue Report 95-001, January 1995.

[9] M.J. Donovan:
EXPERIMENTAL STUDY OF HEAD-DISK INTERFACE DYNAMICS UNDER THE CONDITION OF NEAR-CONTACT RECORDING FOR MAGNETIC DISK DRIVES;
CML Gold Report 95-001, Doctoral Dissertation, May 1995.

[10] M.J. Lipney:
THE DESIGN AND IMPLEMENTATION OF A DIGITAL PHASE DEMODULATOR;
CML Gold Report 90-001, Doctoral Dissertation, 1990.

[11] T.C. McMillan, F.E. Talke:
ULTRA LOW FLYING HEIGHT MEASUREMENTS USING MONOCHROMATIC AND PHASE DEMODULATED LASER INTERFEROMETRY;
IEEE Trans. on Magn., Vol. 30, No. 6, p. 4173, November 1994.

[12] Phase Metrics Corporation:
DFHT - DYNAMIC FLYING HEIGHT TESTER OPERATIONS MANUAL;
Part No. 30, 150 Rev. D, November 1994.

[13] M. Suk:
HEAD-DISK INTERFACE STUDIES IN MAGNETIC DISK DRIVES;
CML Gold Report 91-003, Ph.D. Dissertation, October 1991.

[14] M. Suk, T. Ishii, D.B. Bogy:
COMPARISON OF FLYING HEIGHT MEASUREMENT BETWEEN MULTI-CHANNEL LASER INTERFEROMETER AND CAPACITANCE PROBE SLIDER;
IEEE Trans on Magnetics, Vol. 27, No. 6, pp. 5148 - 5150, November 1991.

[15] M. Tanaka, D.B. Bogy:
EFFECTS OF DISK SURFACE TEXTURE ON SLIDER FLYING CHARACTERISTICS IN THE NEAR CONTACT INTERFACE;
CML Blue Report 94-017, December 1994.

[16] L.Y. Zhu, W.K. Shi, D.B. Bogy:
SIMULTANEOUS MEASUREMENT OF DISK VIBRATIONS AND SLIDER BEARING RESPONSES IN AN OPERATING MAGNETIC DISK FILE;
Tribology and Mechanics of Storage Systems, Vol. III, ASLE Sp-21, 1986.

[17] L.Y. Zhu, K.F. Hallamasek, D.B. Bogy:
MEASUREMENT OF HEAD/DISK SPACING WITH A LASER INTERFEROMETER;
IEEE Trans on Magnetics, Vol. 24, No 6, November 1988.

[18] L.Y. Zhu:
MEASUREMENT AND ANALYSIS OF THE SLIDER DISK SPACING IN MAGNETIC RECORDING DISK FILES;
CML Gold Report, Doctoral Dissertation, 1989.

[19] L.Y. Zhu, D.B. Bogy:
A MULTI-CHANNEL LASER INTERFEROMETER AND ITS USE TO STUDY HEAD-DISK INTERFACE DYNAMICS IN MAGNETIC DISK FILES;
Tribology and Mechanics of Magnetic-Storage Systems, STLE SP-26, 1989.

[20] ZYGO Corporation:
AXIOM 2/20 LASER MEASUREMENT SYSTEM OPERATION AND REFERENCE MANUAL;
Version OMP-0220F, 1990.

7. Figures

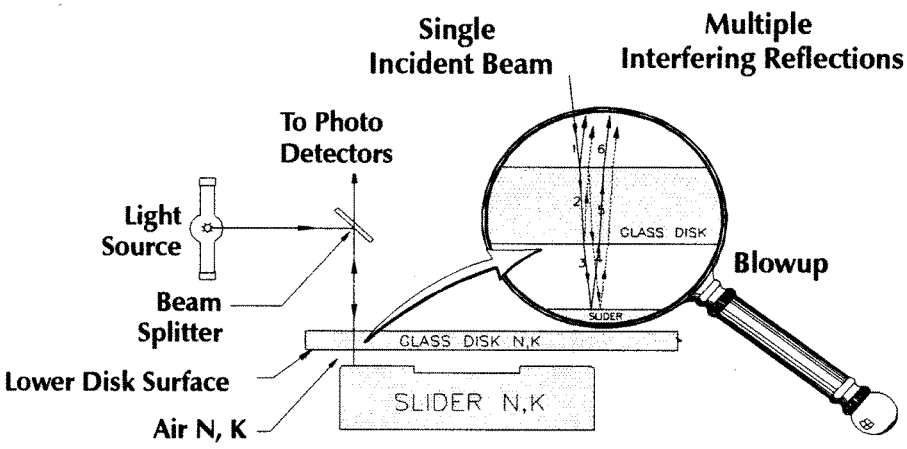

Figure 2.1: Light path in the Phase Metrics DFHT

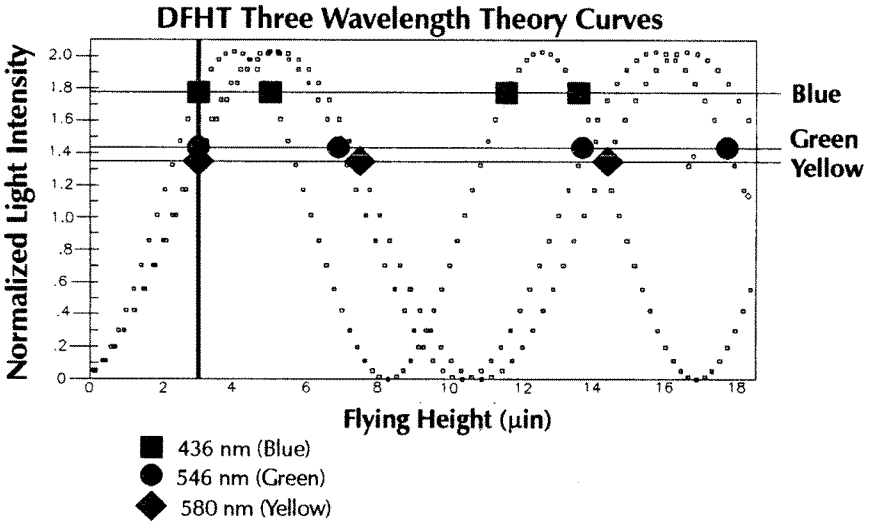

Figure 2.2: Theoretical intensity curves for the three wavelengths in DFHT

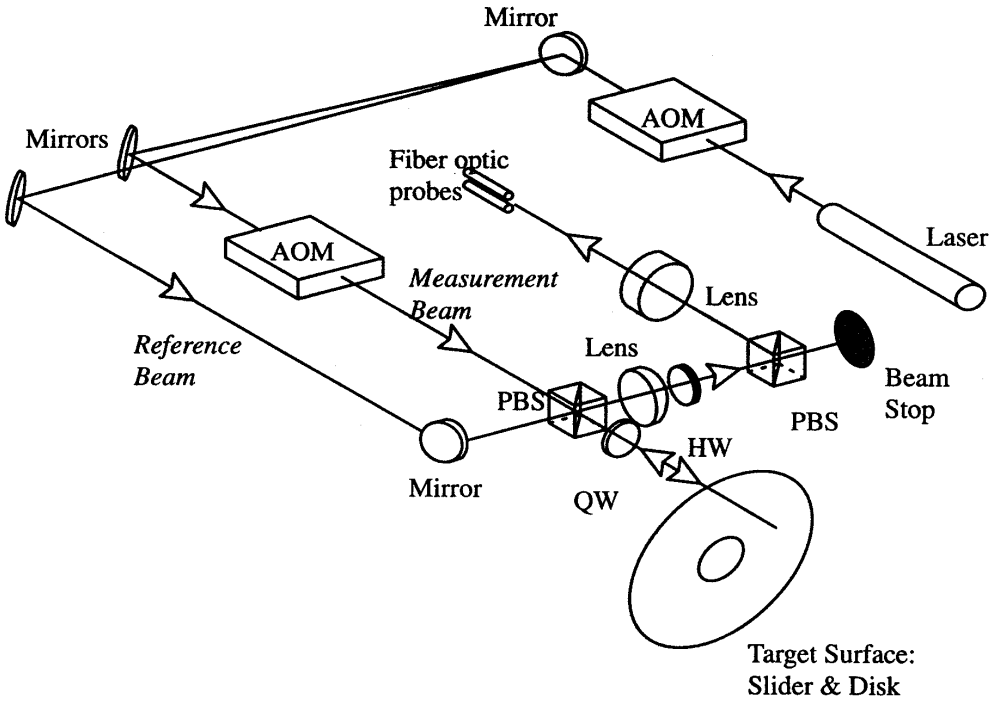

Figure 2.3: Optical layout for the MCLI

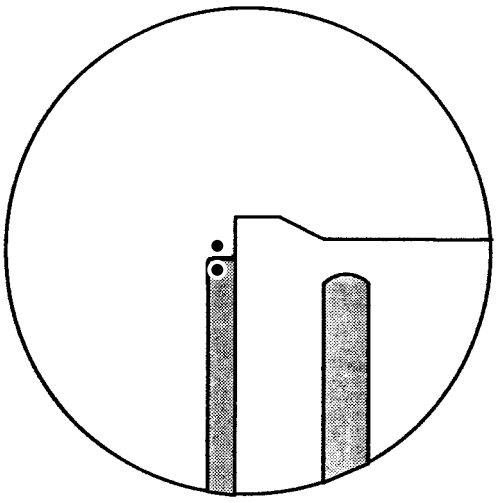

Figure 2.4: Slider and disk in the image plane
Two fibre optic probes are indicated by black dots

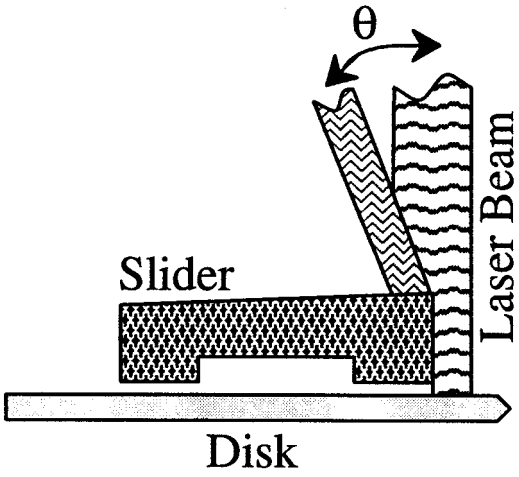

Figure 2.5: Divergent reflections if the slider is not parallel to the disk

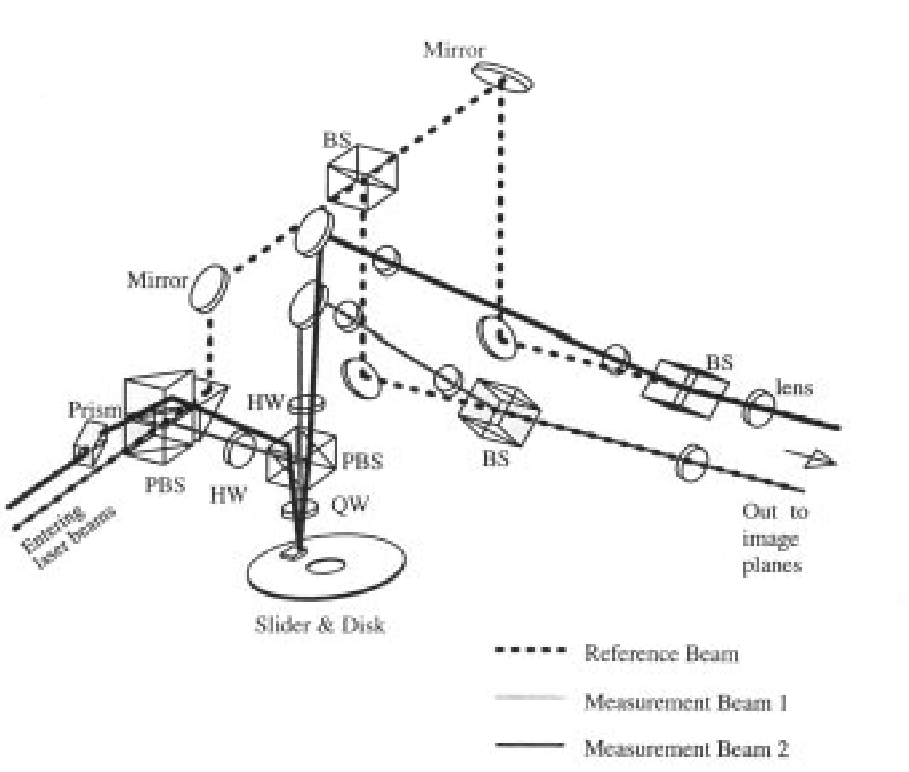

Figure 2.6: Optical setup in the BALI system

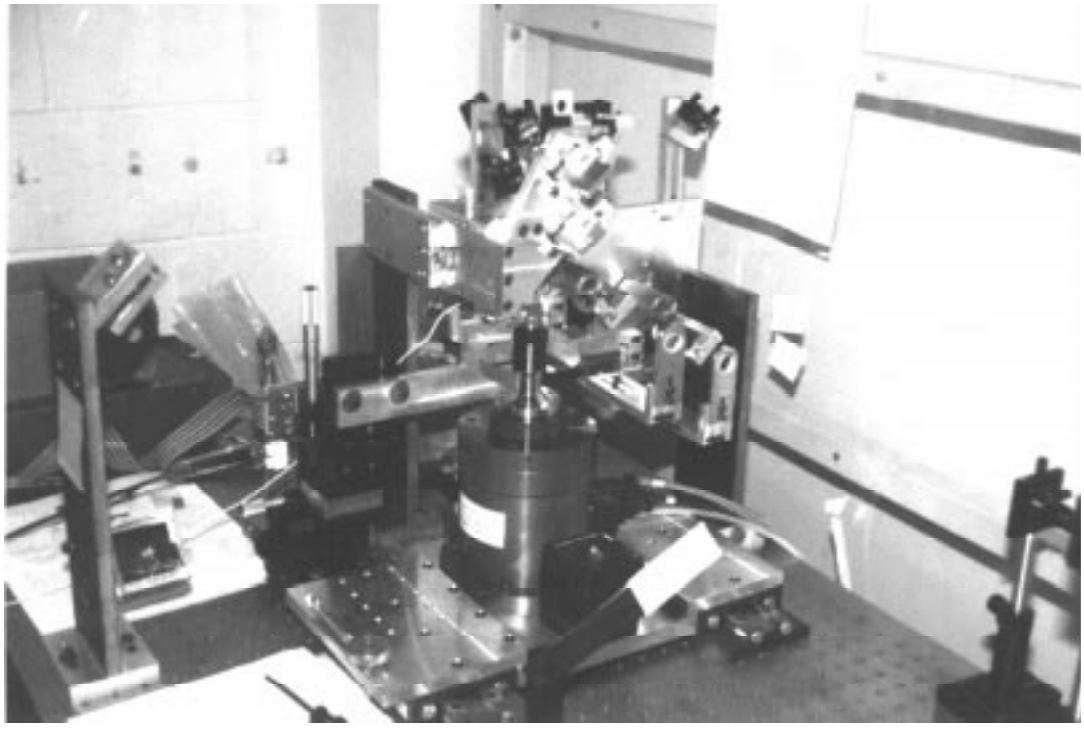

Figure 2.7: Optical setup in the BALI system

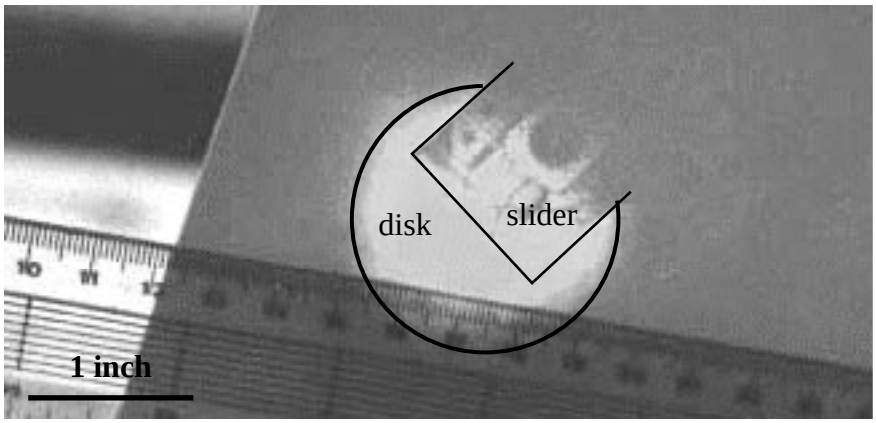

Figure 2.8: View of the image plane (slider and disk)

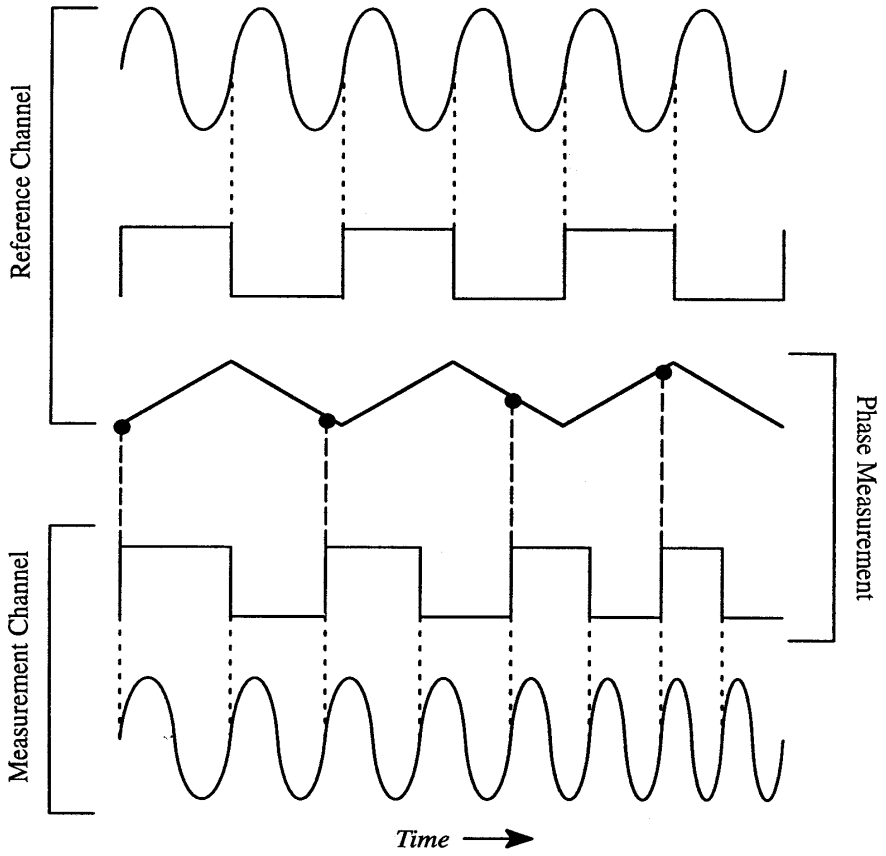

Figure 2.9: Demodulation scheme in the ZYGO Axiom 2/20

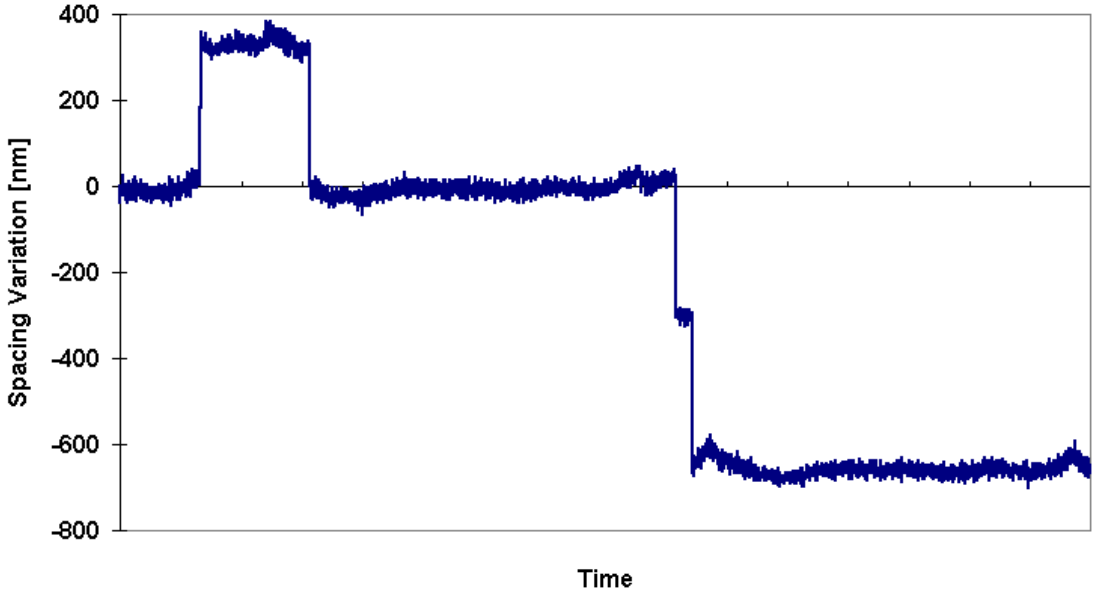

Figure 2.10: "Jumps" (± 316.4 nm) in the displacement signal from BALI

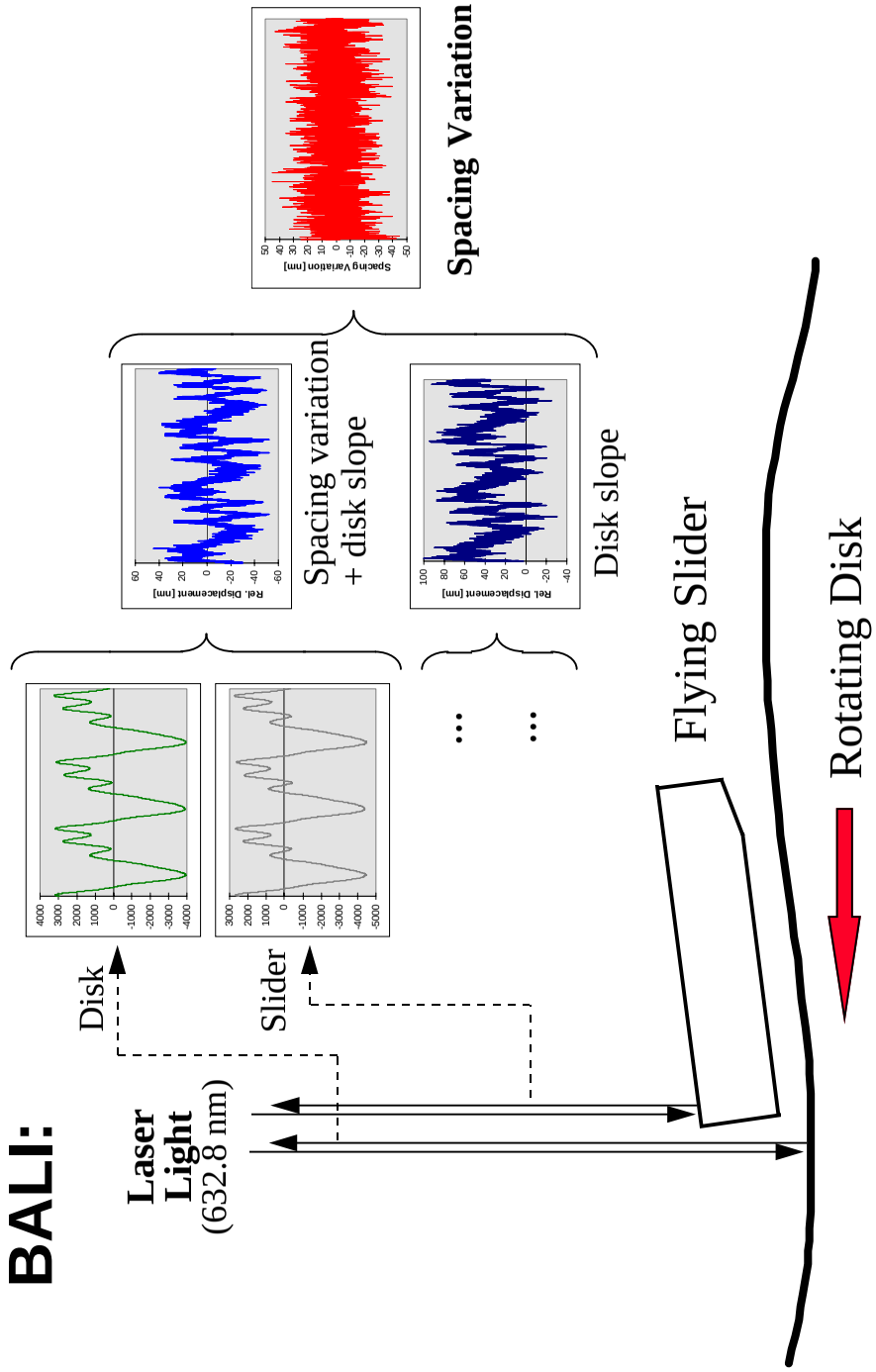

Figure 2.11: Procedure to measure the spacing variation with the BALI system

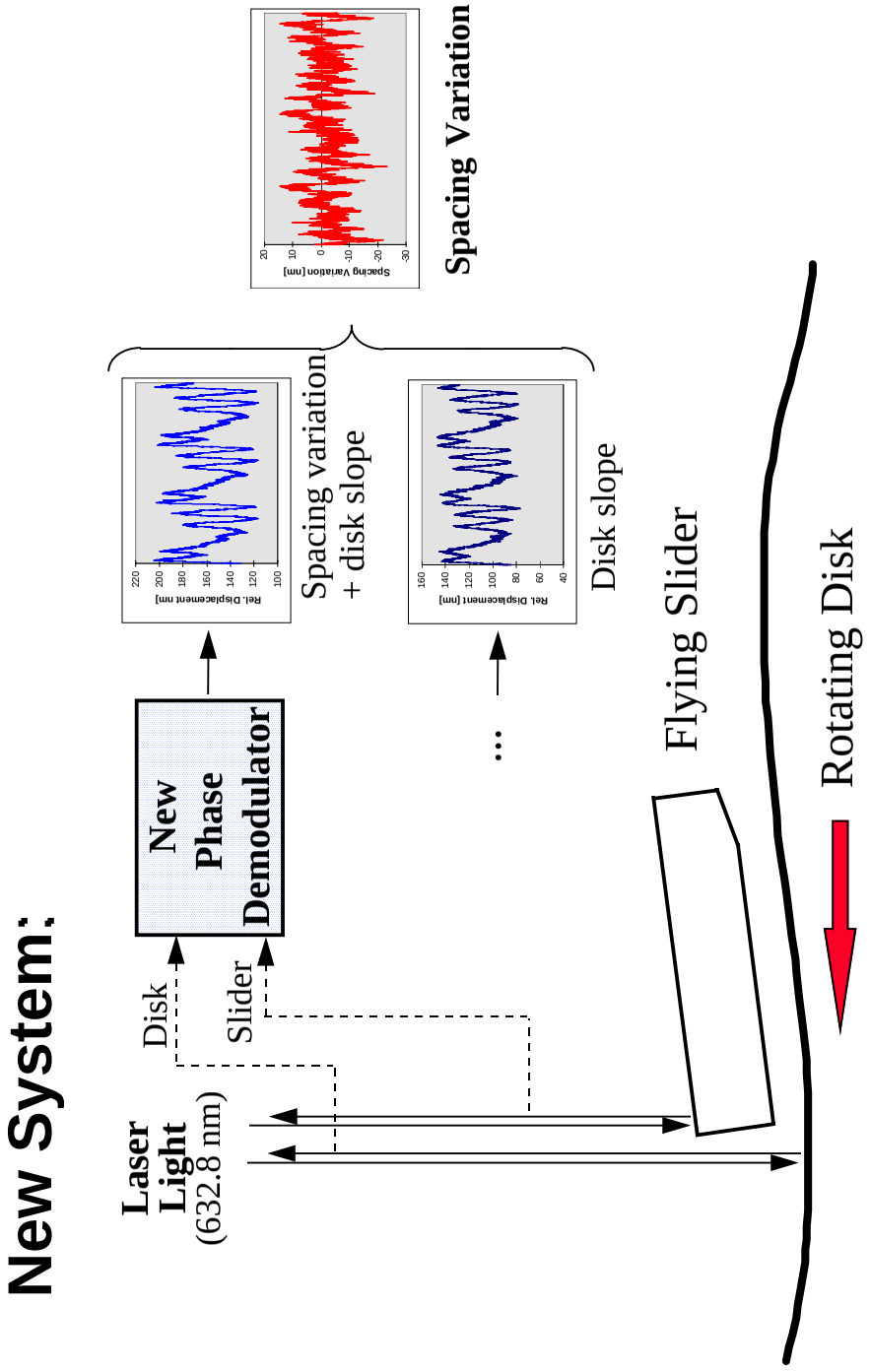

Figure 3.1: Procedure to measure the spacing variation with the new system

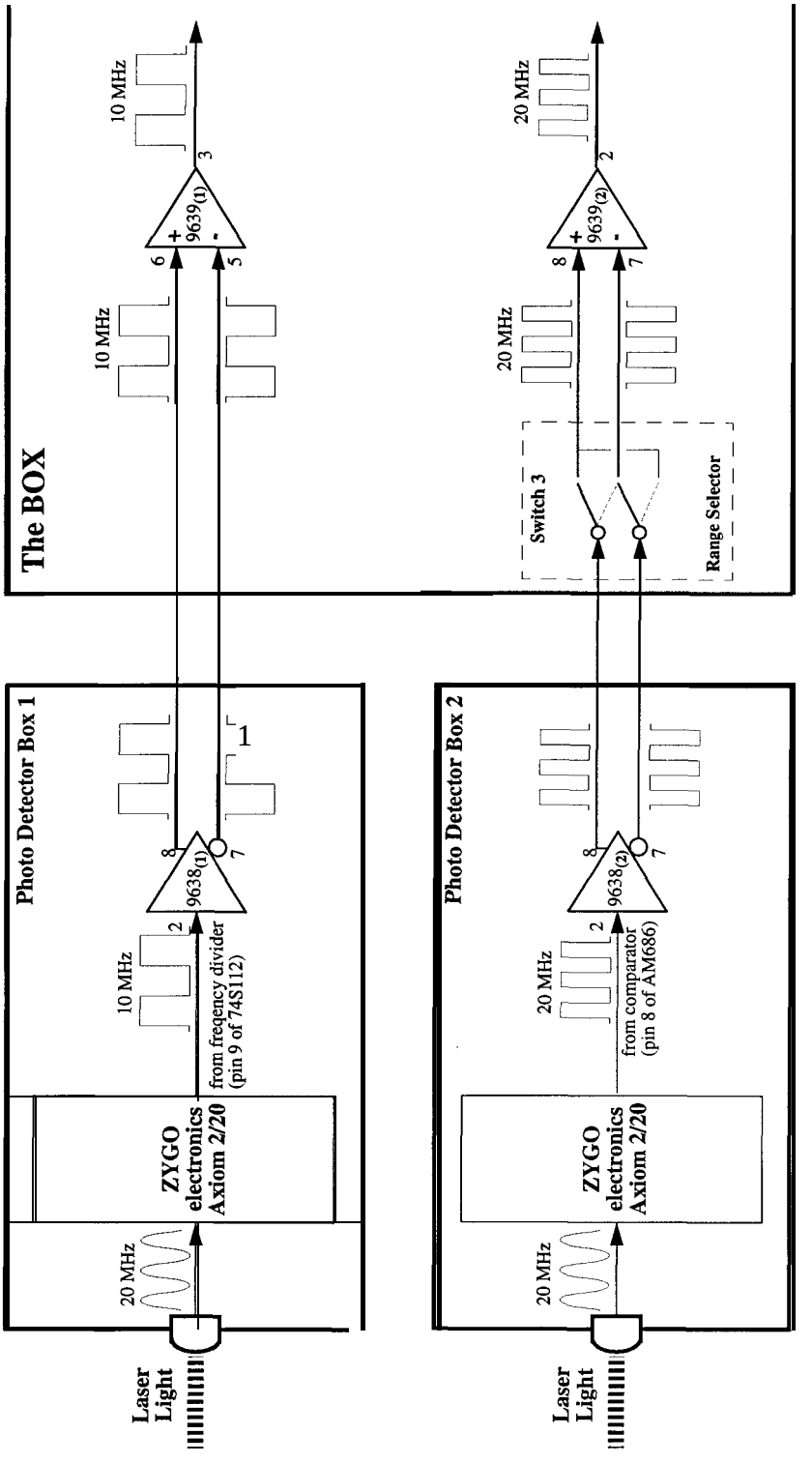

Figure 3.2: Data Transfer between Photodetector Boxes and new Circuit

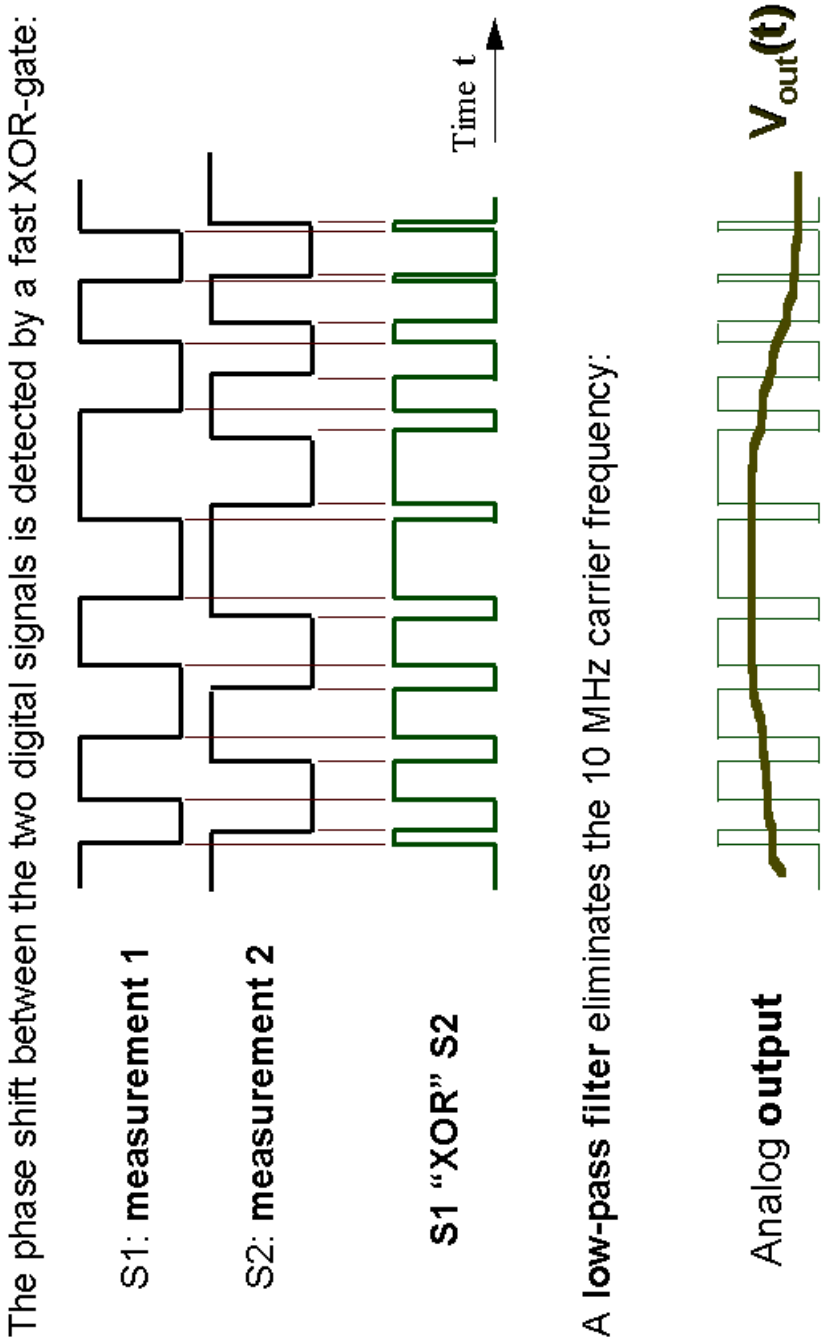

Figure 3.3: Phase Detector used in the new System

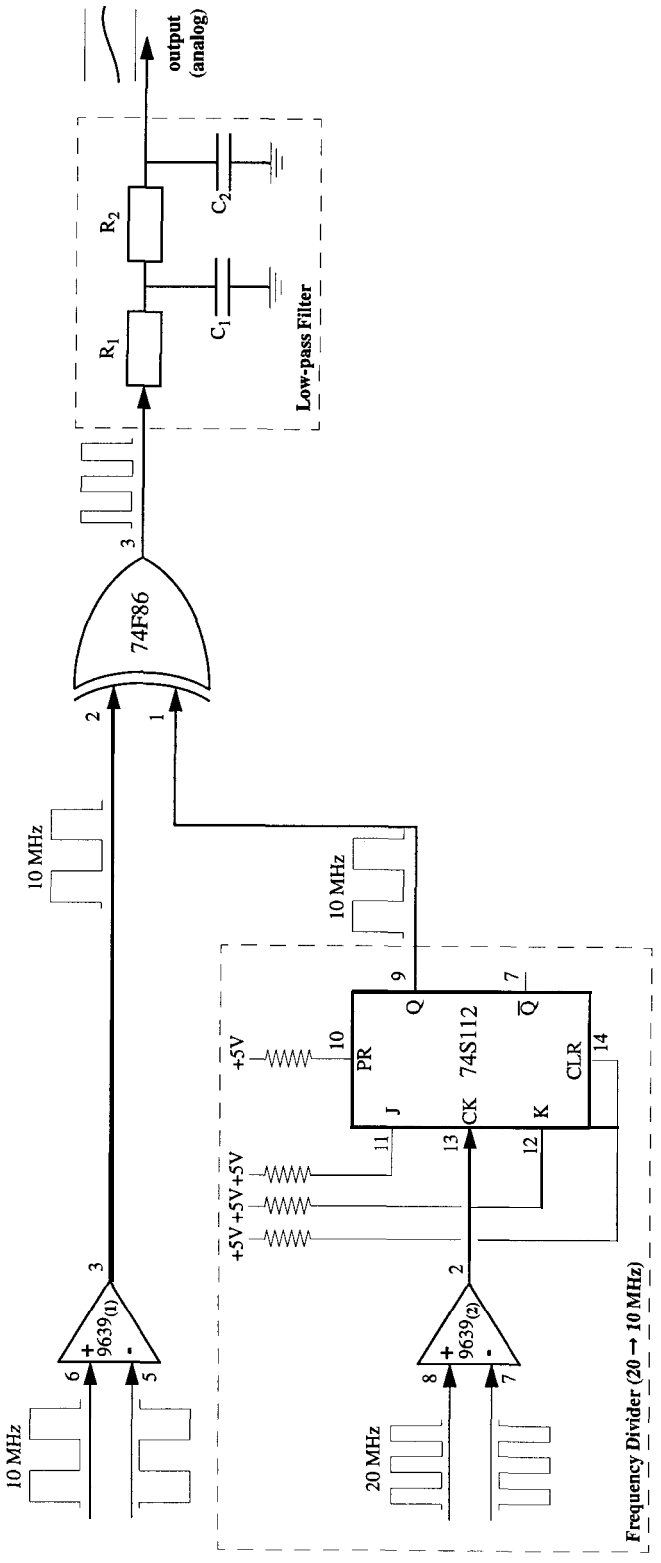

Figure 3.4: Electronic Circuit: Main Parts

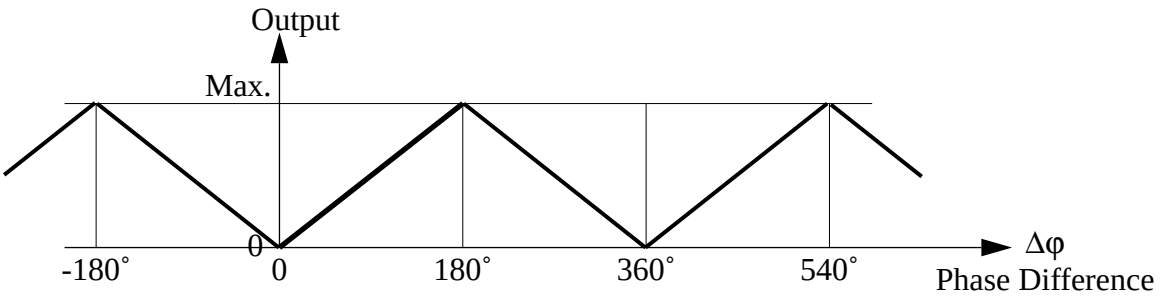

a) Output (averaged) of the XOR phase detector: Before modification

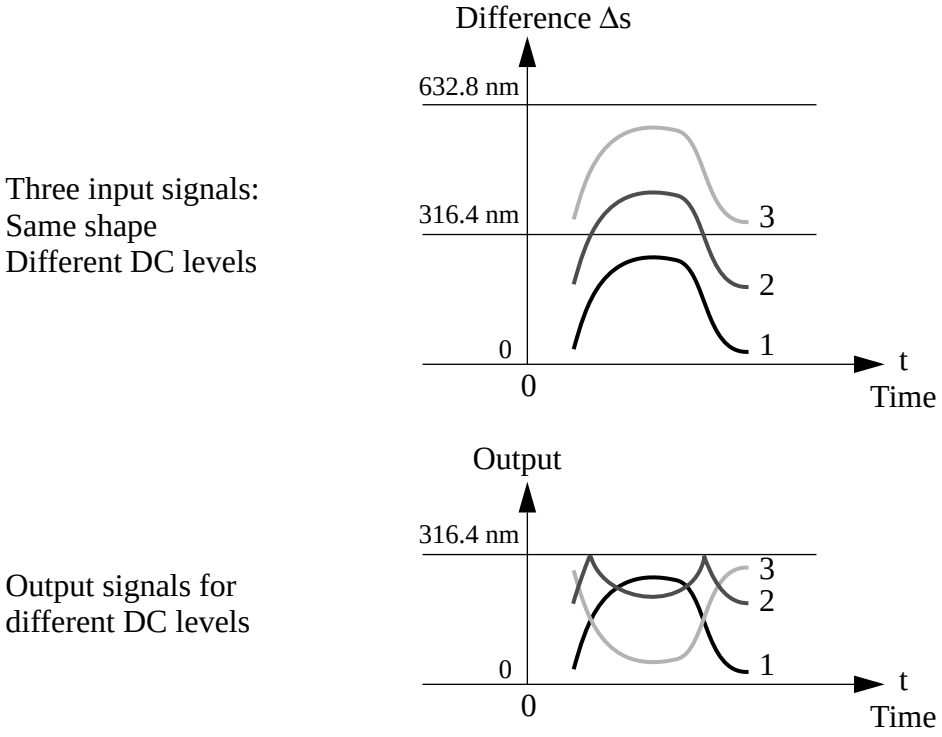

b) Output for signals for different DC levels of Δs(t)

Figure 3.5: Transfer Function of an XOR Phase Detector

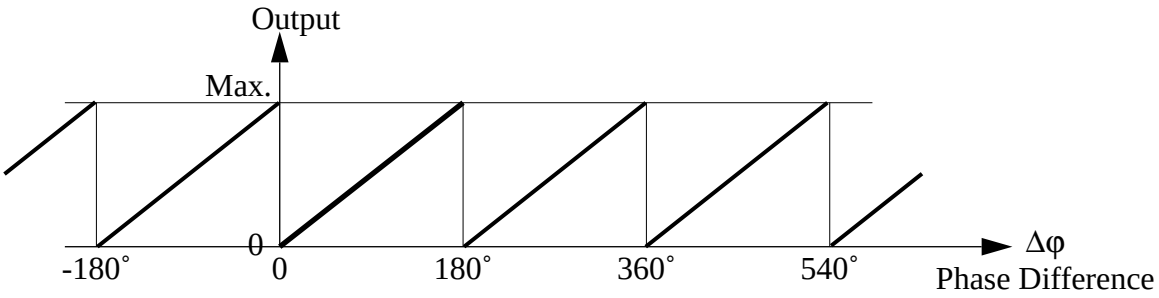

a) Output (averaged) of the phase detector: After modification

Three input signals:
Same shape
Different DC levels

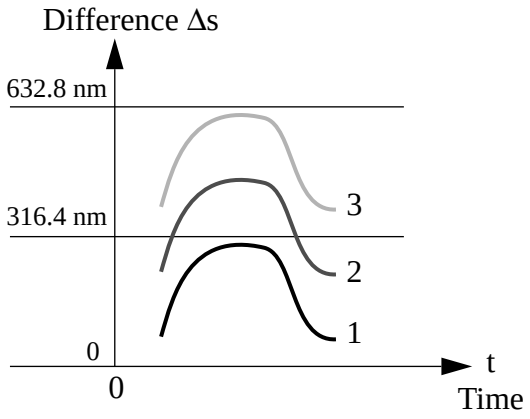

Output signals for
different DC levels

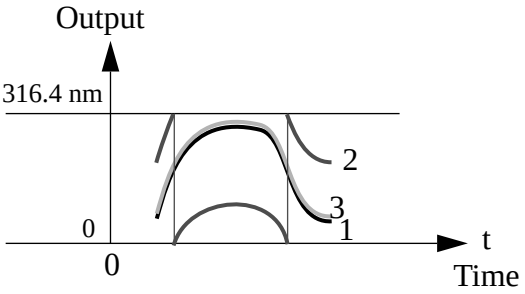

b) Output for signals for different DC levels of Δs(t)

Figure 3.6: Transfer Function of the modified XOR Phase Detector

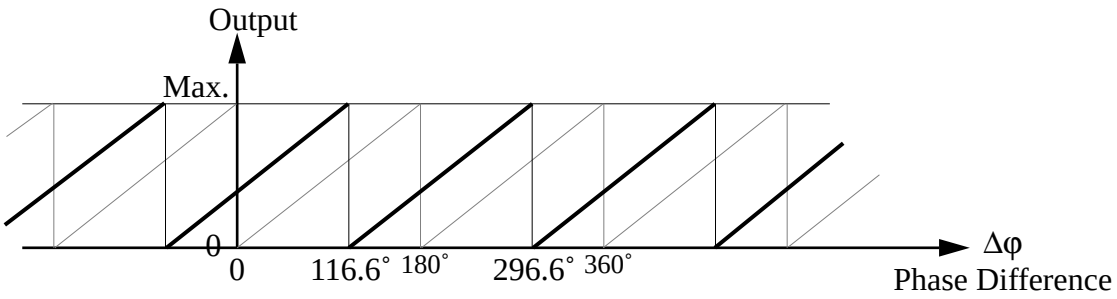

a) Transfer function of the phase detector: Shifted measurement range

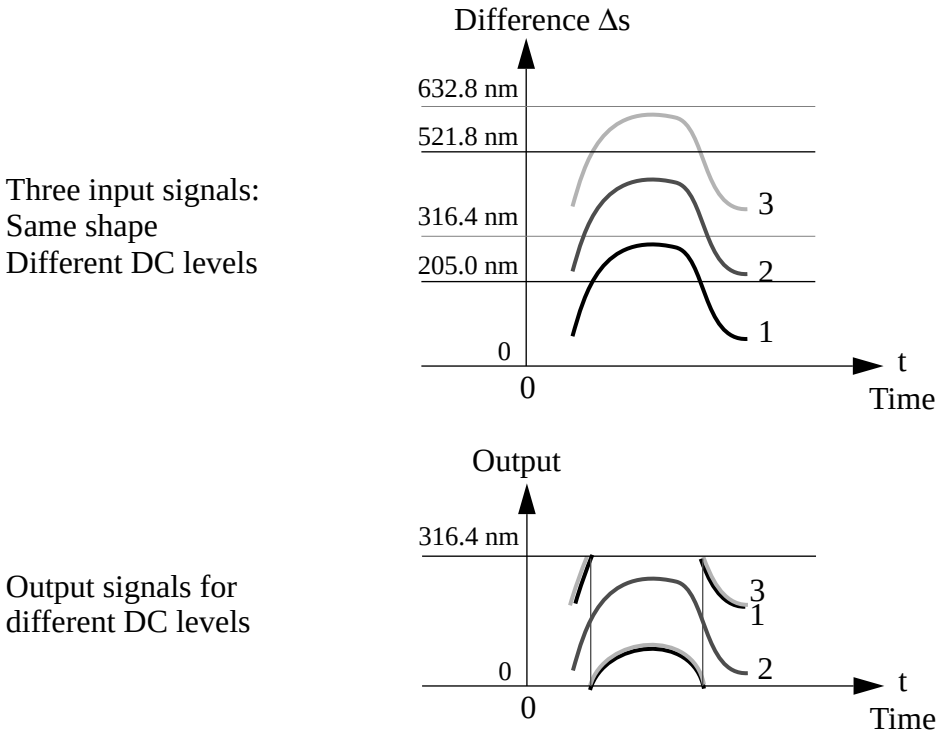

b) Output for signals for different DC levels of Δs(t)

Figure 3.7: Transfer function of the Phase Detector: Shifted Measurement Range

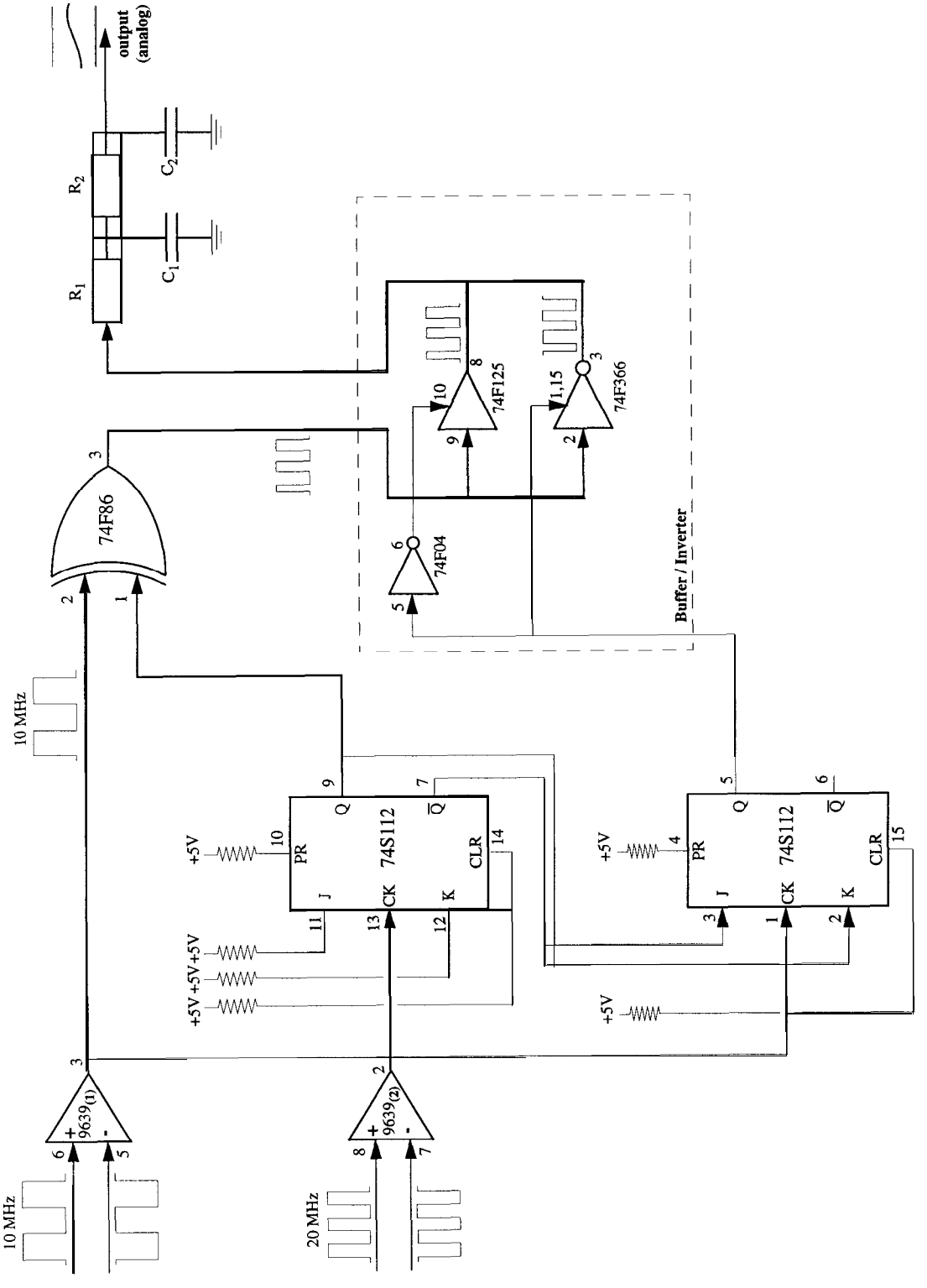

Figure 3.8: Output Buffer / Inverter

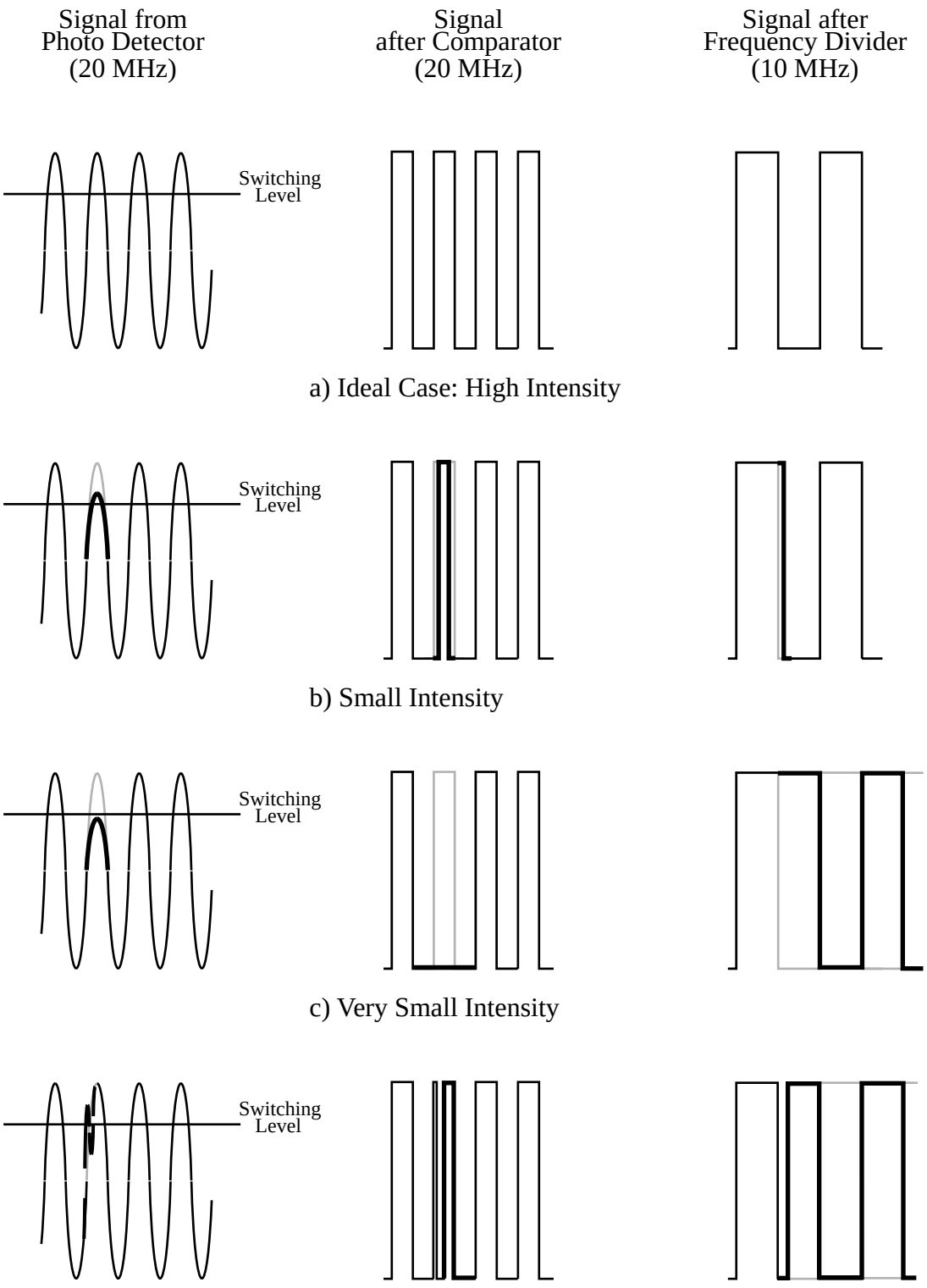

Figure 3.9: Errors caused by weak light intensity
(exaggerated for clarity)

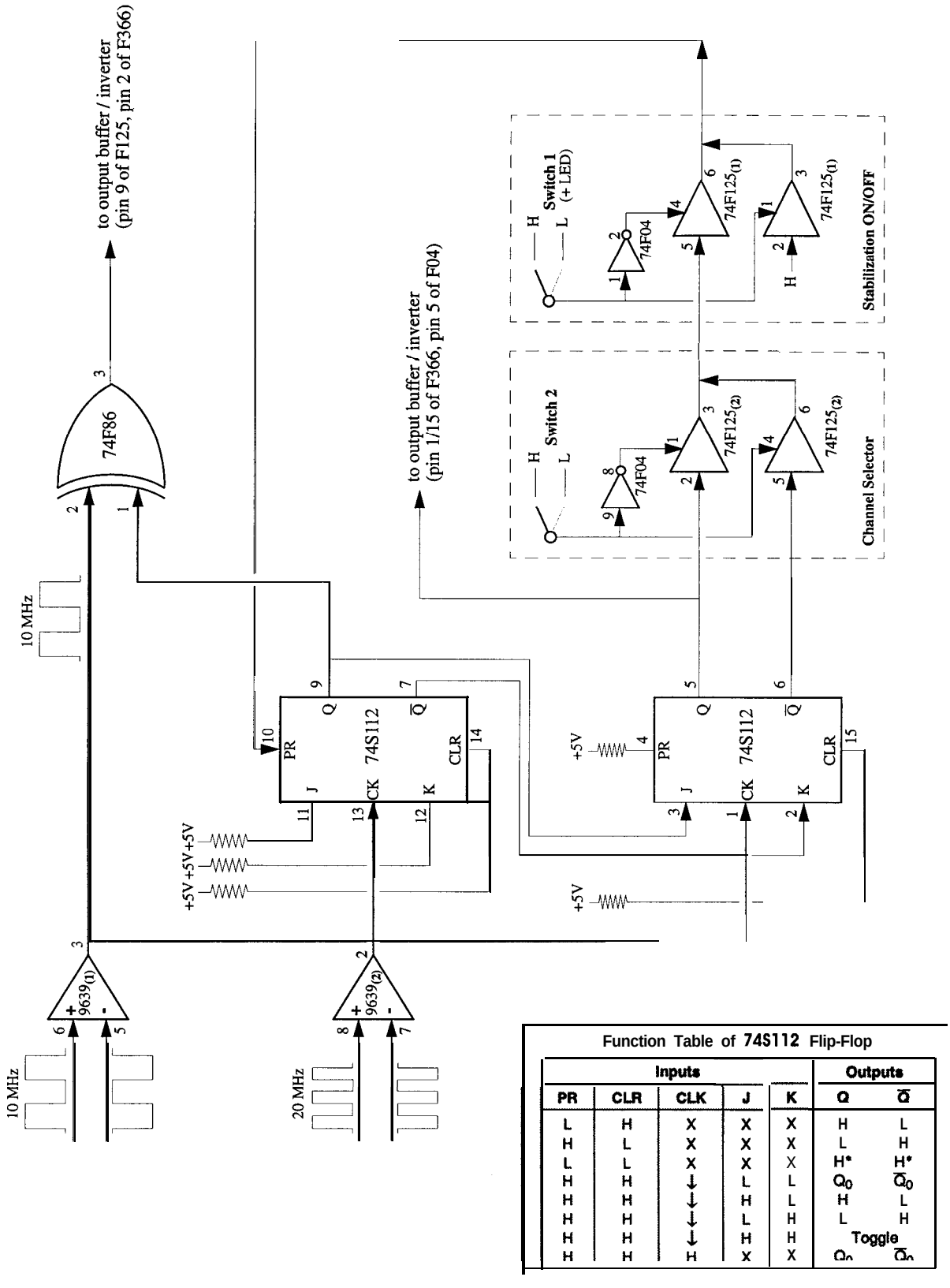

Function Table of 74S112 Flip-Flop

Inputs					Outputs	
PR	CLR	CLK	J	K	Q	Q̄
L	H	X	X	X	H	L
H	L	X	X	X	L	H
L	L	X	X	X	H*	H*
H	H	↓	L	L	Q_0	$\bar{Q}_0$
H	H	↓	H	L	H	L
H	H	↓	L	H	L	H
H	H	↓	H	H	Toggle	
H	H	H	X	X	Q_0	$\bar{Q}_0$

Figure 3.10: Signal Stabilization and Channel Selection

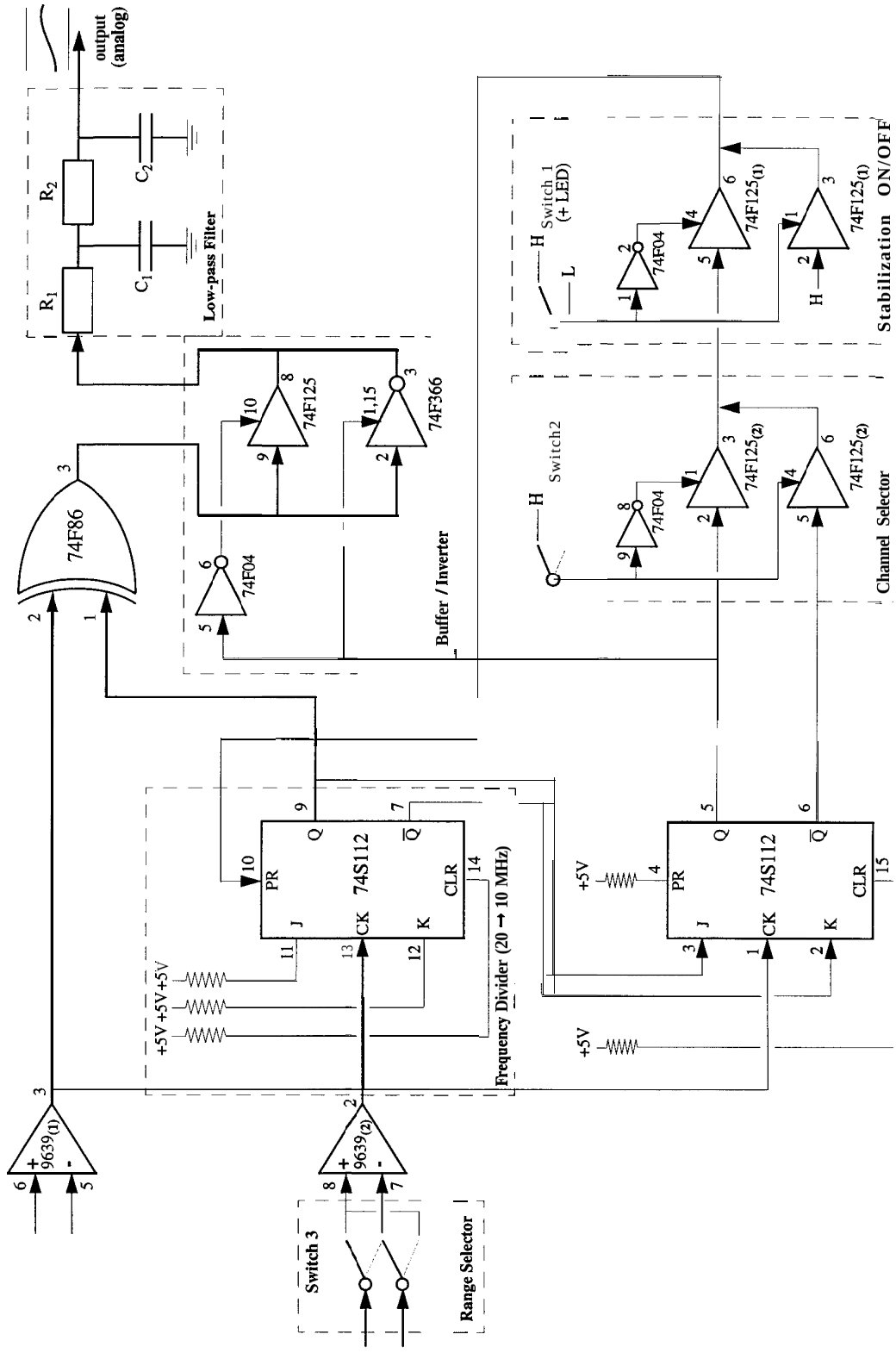

Figure 3.11: Full Circuit

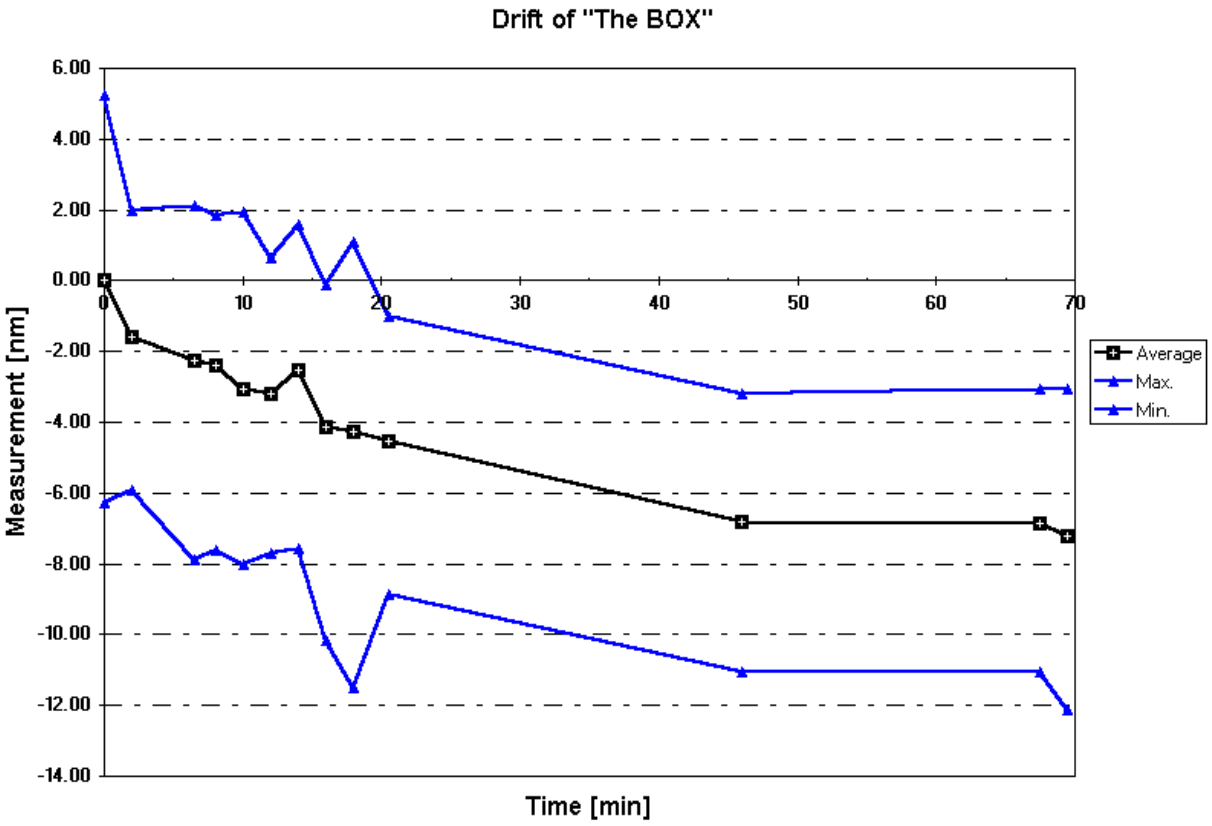

Figure 3.12: Drift: DC level for a resting target as a function of time

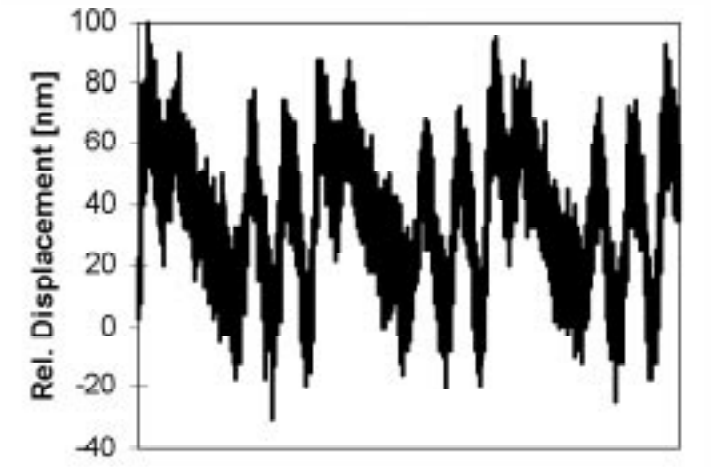

a) Measurement using the BALI system

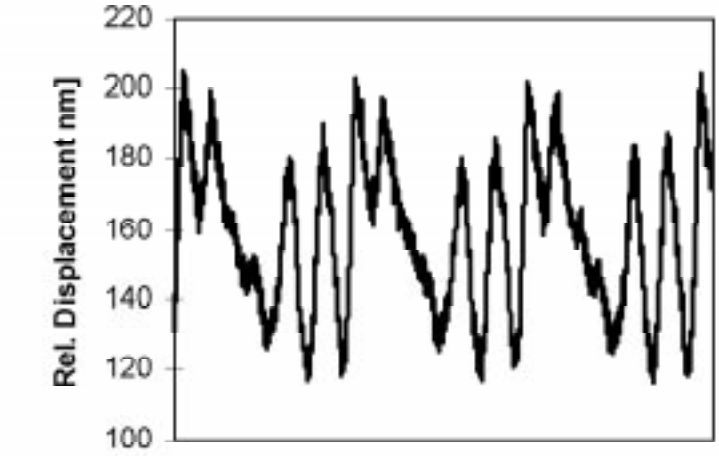

b) Measurement using the new system

Figure 4.1: Measurement of the Disk Slope

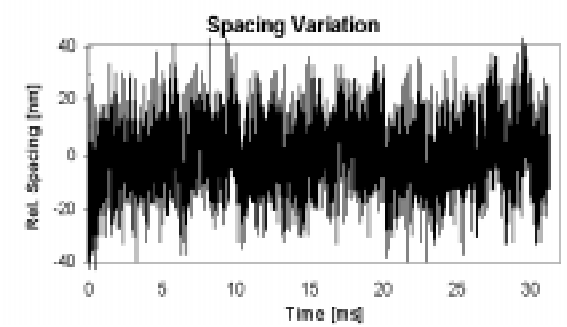

a) Measurement using the BALI system

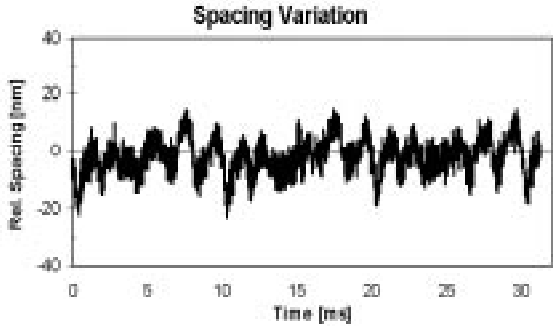

b) Measurement using the new system

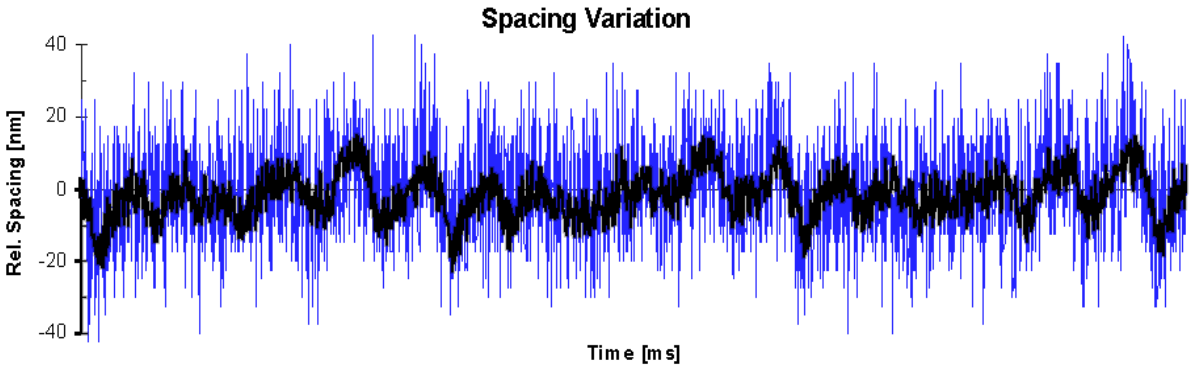

c) Comparison of measurements a) and b)

Figure 4.2: Measurement of the Spacing Variation

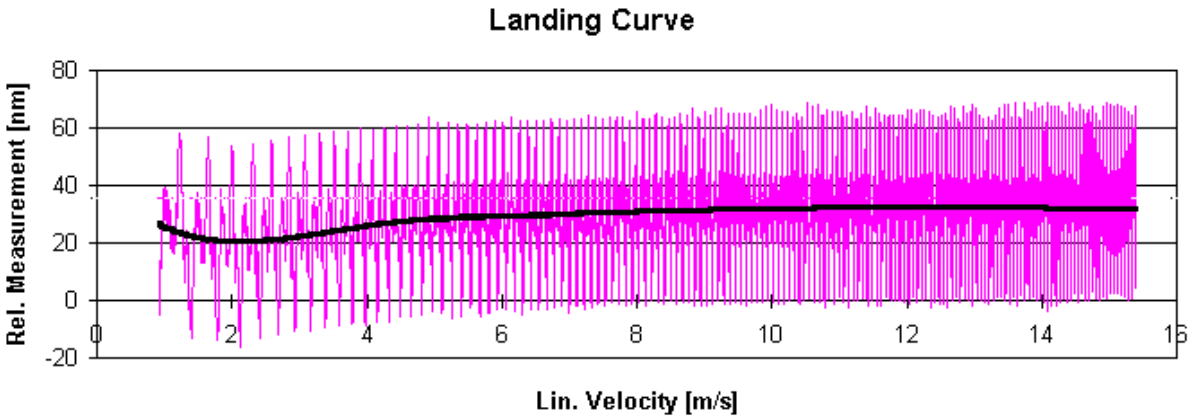

Figure 4.3: Landing Curve: Direct measurement
(AAB over textured disk)

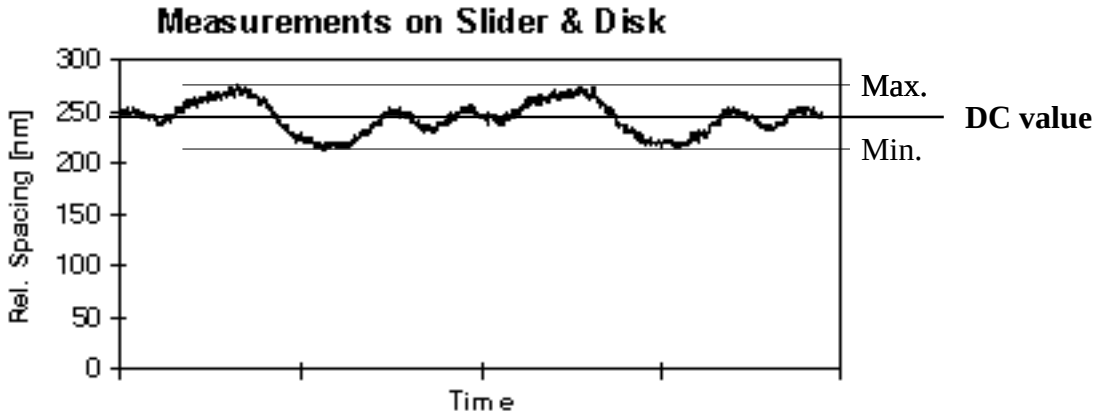

Figure 4.4: Determination of one data point in the landing curve

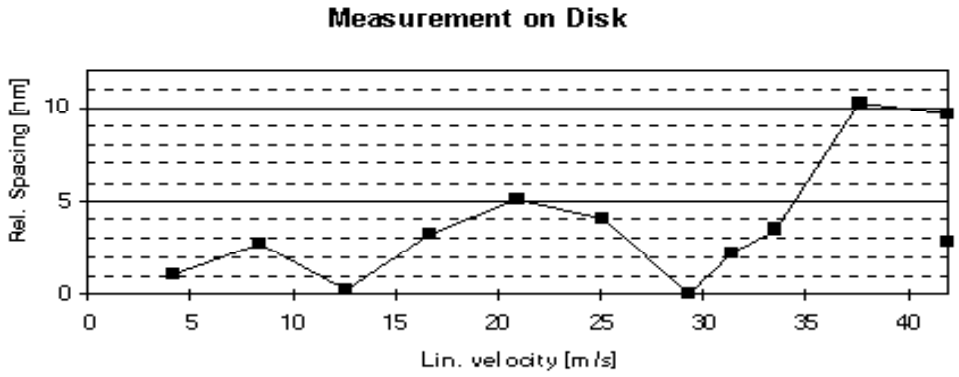

Figure 4.5: Measurement on disk

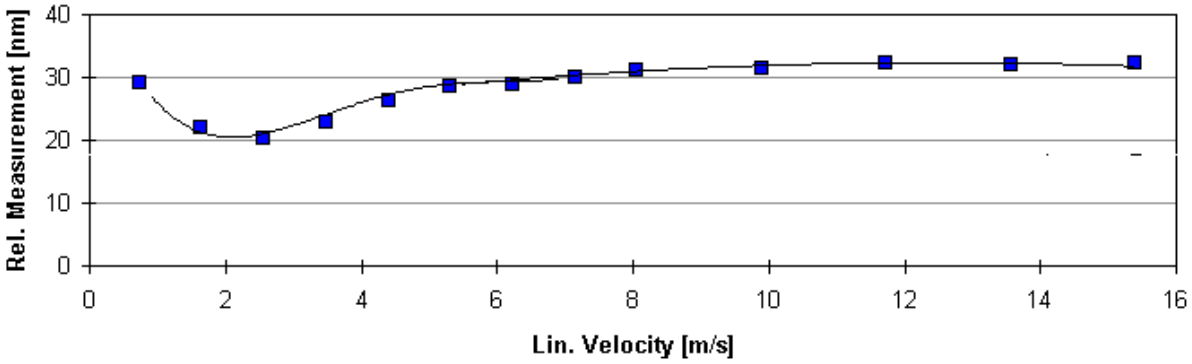

Figure 4.6: Comparison of two measurements:
Direct Measurement (smoothed; solid line)
DC values at different velocities (squares)
(AAB over textured disk)

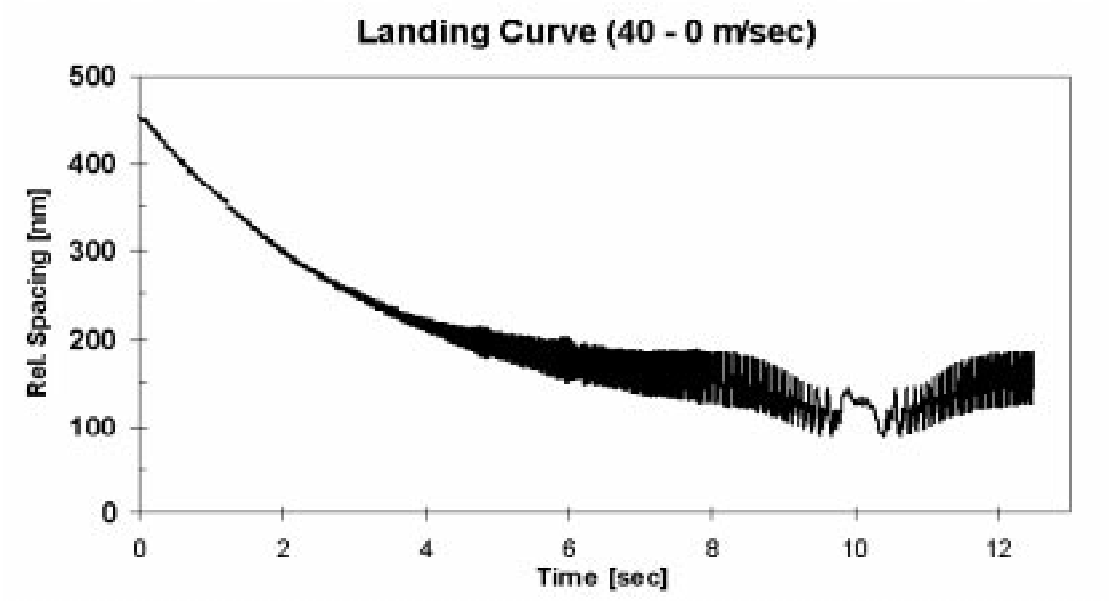

Figure 4.7: Large Landing Curve: Direct measurement
(start at 40 m/s, stop after 10 seconds)
(large flying height due to bad slider)

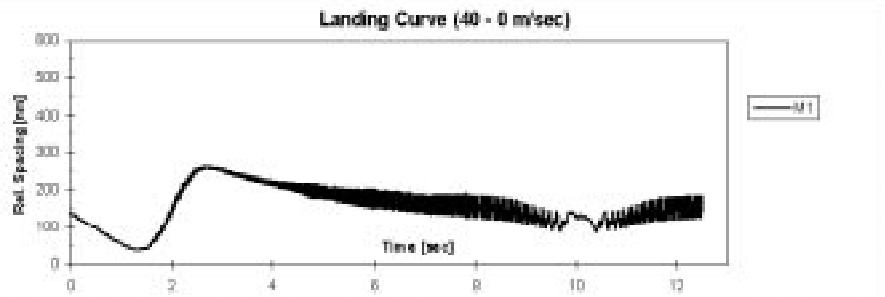

a) Measurement M1: Direct Output

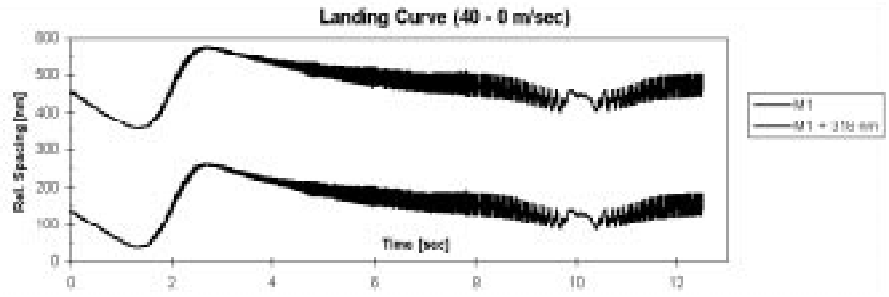

b) Measurement M1: Output shifted by 316.4 nm

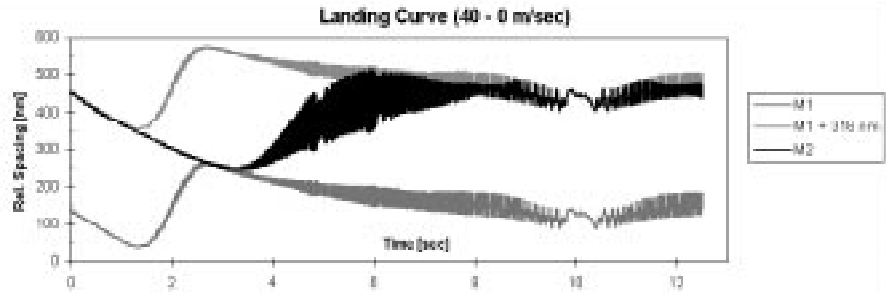

c) Measurement M2: Range Shifted

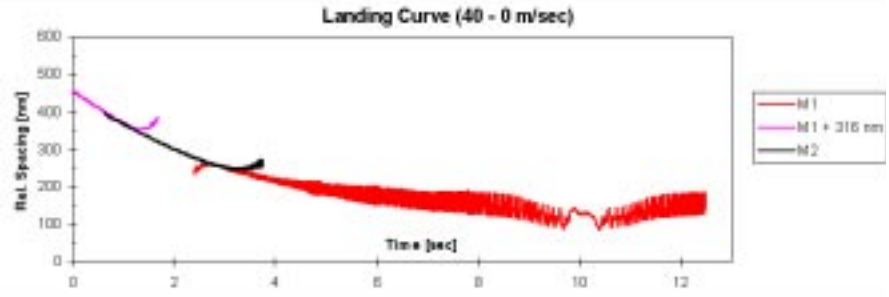

d) Combination of 3 signals (M1, M1+316.4nm, M2)

Figure 4.8: Measurement of a large signal

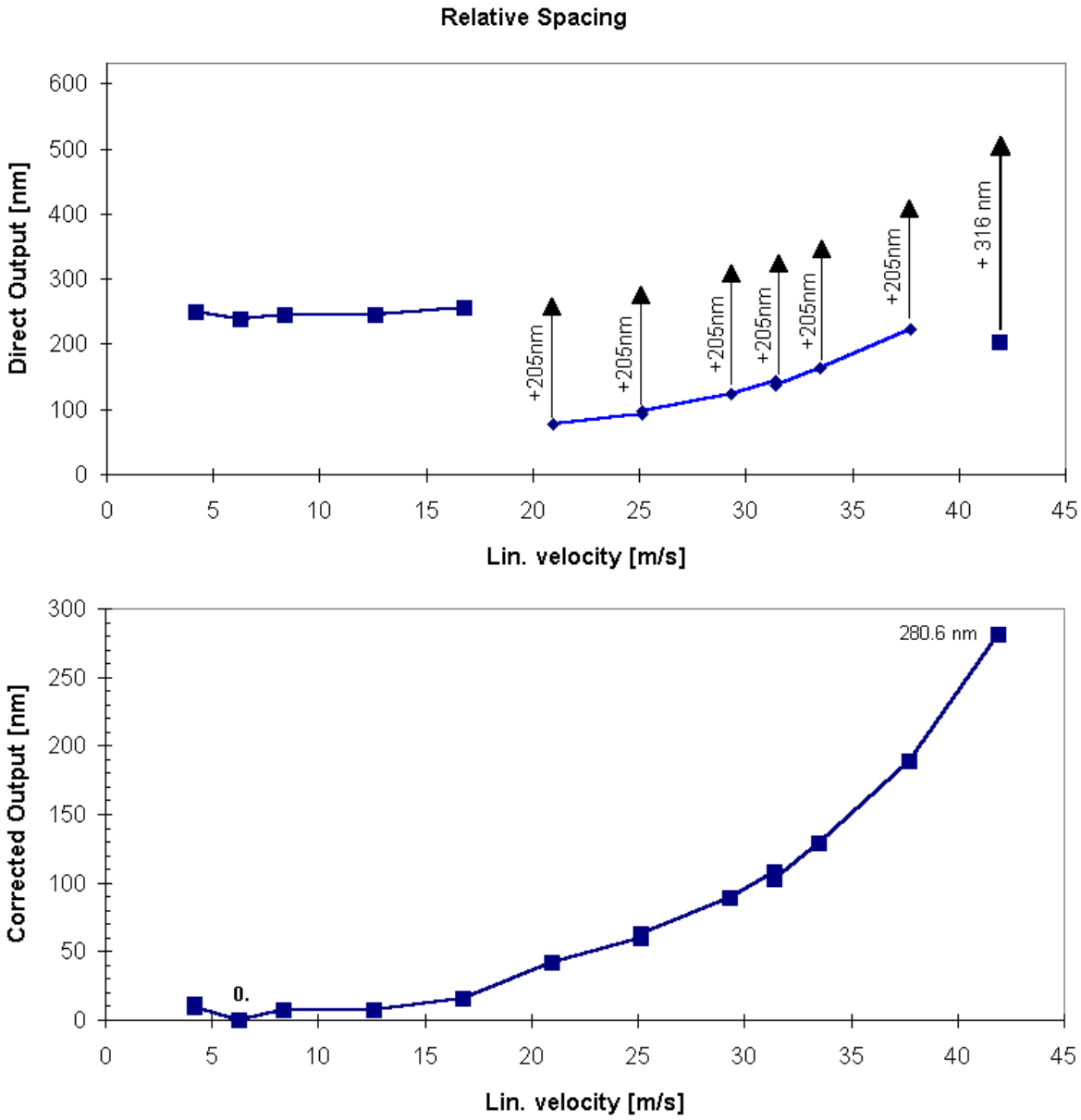

Figure 4.9: Large Landing Curve: Combination of several measurements
top: output as measured
bottom: corrected (+205 or +632 nm)
(large flying height due to bad slider)

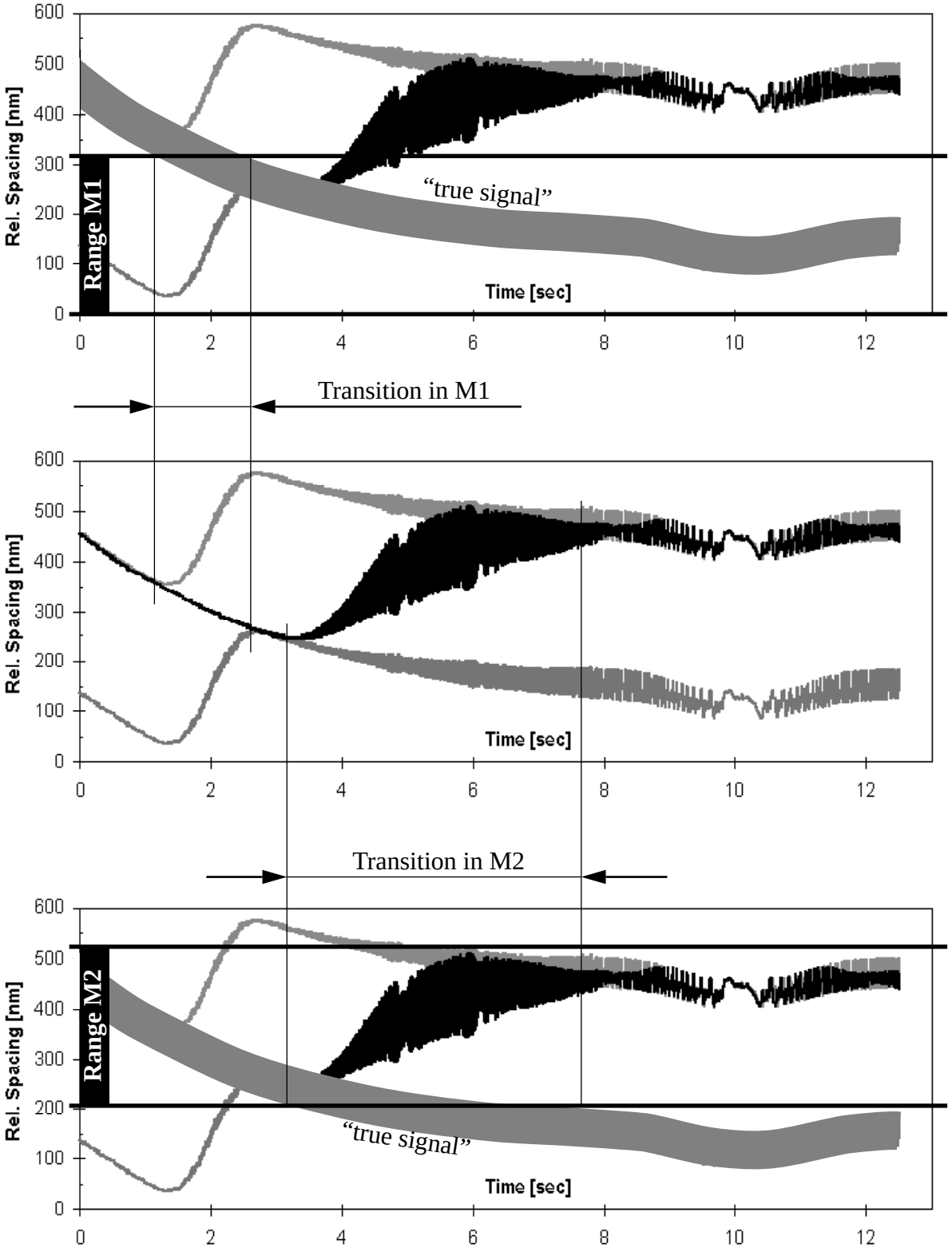

Figure 4.10: Transition in output signal if displacement exceeds measurement range